Stochastic acceleration and the evolution of spectral distributions in SSC sources: A self consistent modeling of TeV blazars' flares

Tramacere A., Massaro E., & Taylor A.,   2011ApJ...739...66T

Andrea Tramacere - ISDC

collaborators: Enrico Massaro, Andrew Taylor

Gamma 2012

Heidelberg, 11-Jul-2012

OUTLINE

The aim of this talk is to provide a self-consistent explanation of the X-ray spectral phenomenology of TeV blazars, in terms of a stochastic acceleration scenario. **Our analysis bases on interpretation of the spectral curvature, in terms of a stochastic acceleration signature**

main topics:

- phenomenological approach: acceleration signatures in the X-ray log-parabolic spectral trends

- log-parabola physical insight: statistical derivation, and diffusion equation derivation

- self-consistent approach: numerical modeling of particle and SED evolution resulting from the competition between acceleration and radiative losses

- model vs observed X-ray trends and γ-ray predictions

- conclusions

Phenomenological approach

LP SPECTRAL DISTRIBUTION OF HBLs

E. Massaro et al.: The log-parabolic X-ray spectra of Mkn 501

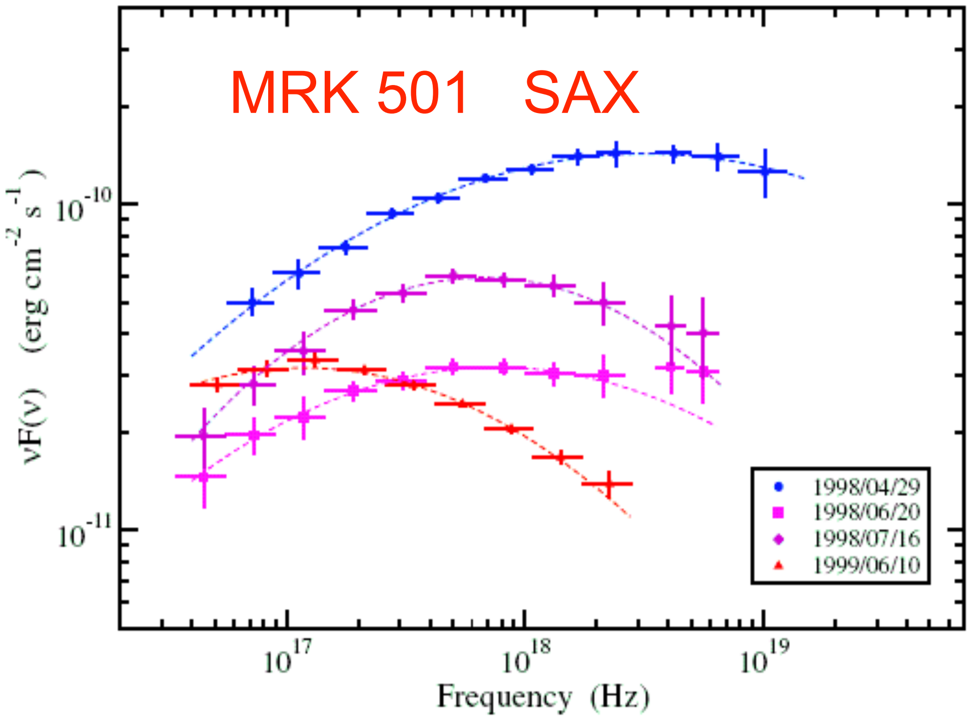

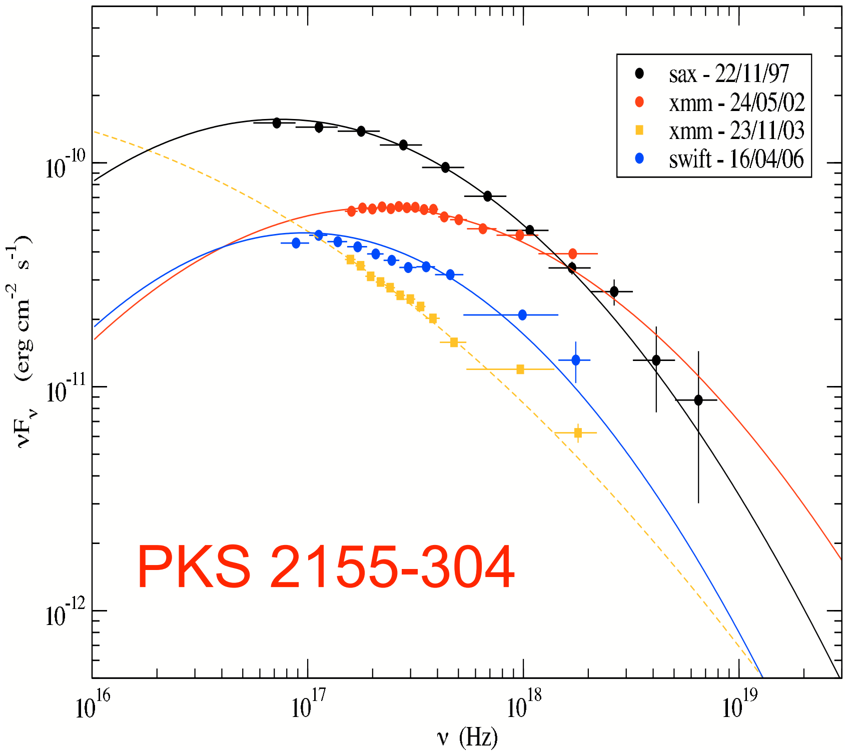

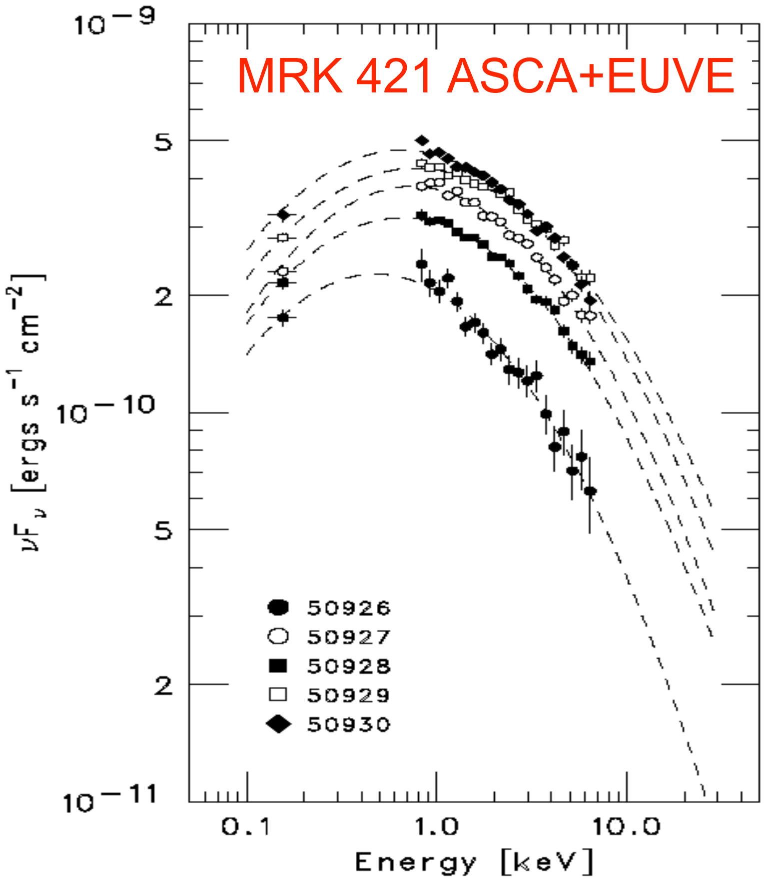

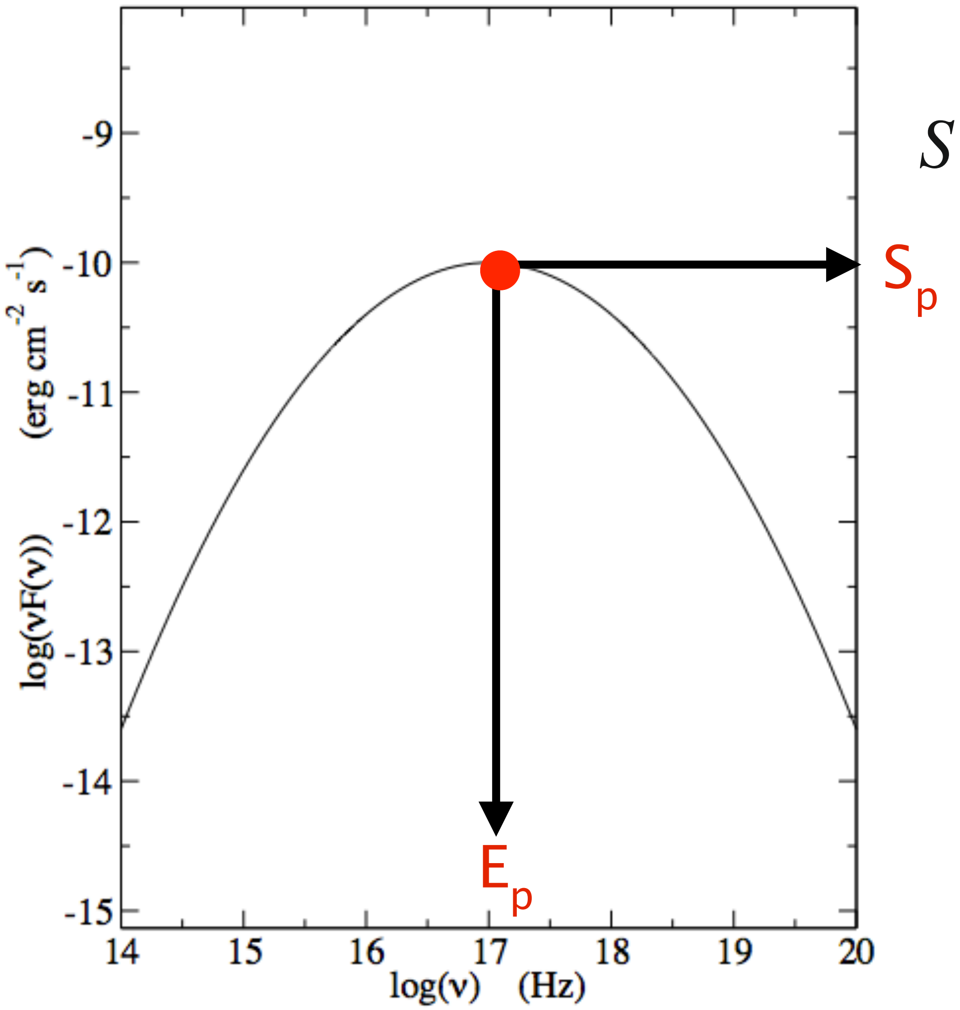

$$S(E) = S_{\rm p}\, 10^{-b\ (\log(E/E_{\rm p}))^2}$$

- b: curvature at peak
- E_p: peak energy
- S_p: SED height @ E_p

•UV to hard-X-ray SEDs of HBLs are well fitted by log-parabolic distributions,
•hinting for an “intrinsic” spectral curvature in the underlying electron energy distribution

acceleration signature in the E_S-vs-b trend

Tramacere A., et al., 2007A&A...466 AND 2009A&A...501

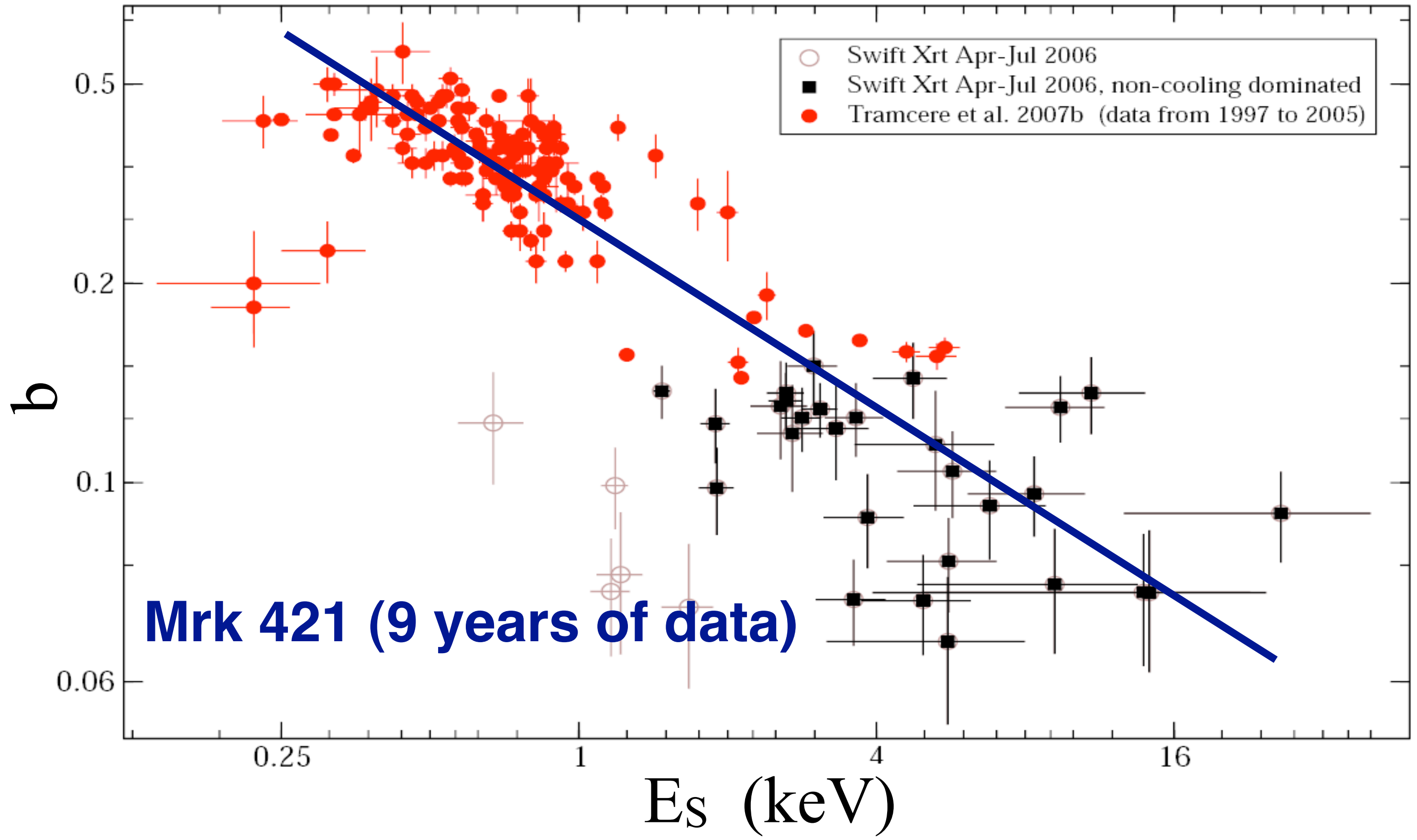

Massaro F., Tramacere A., et al., 2007 A&A...488

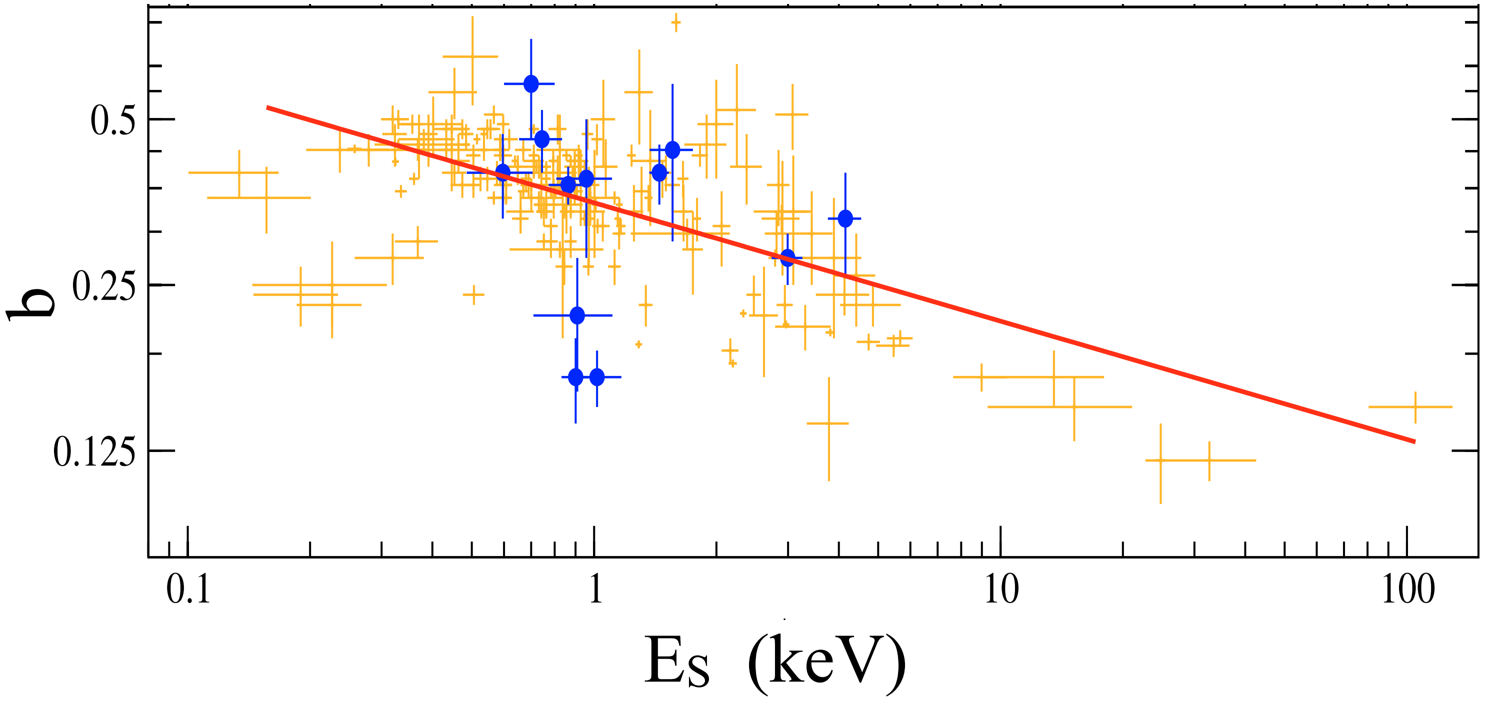

Ep-vs-b, different scenarios

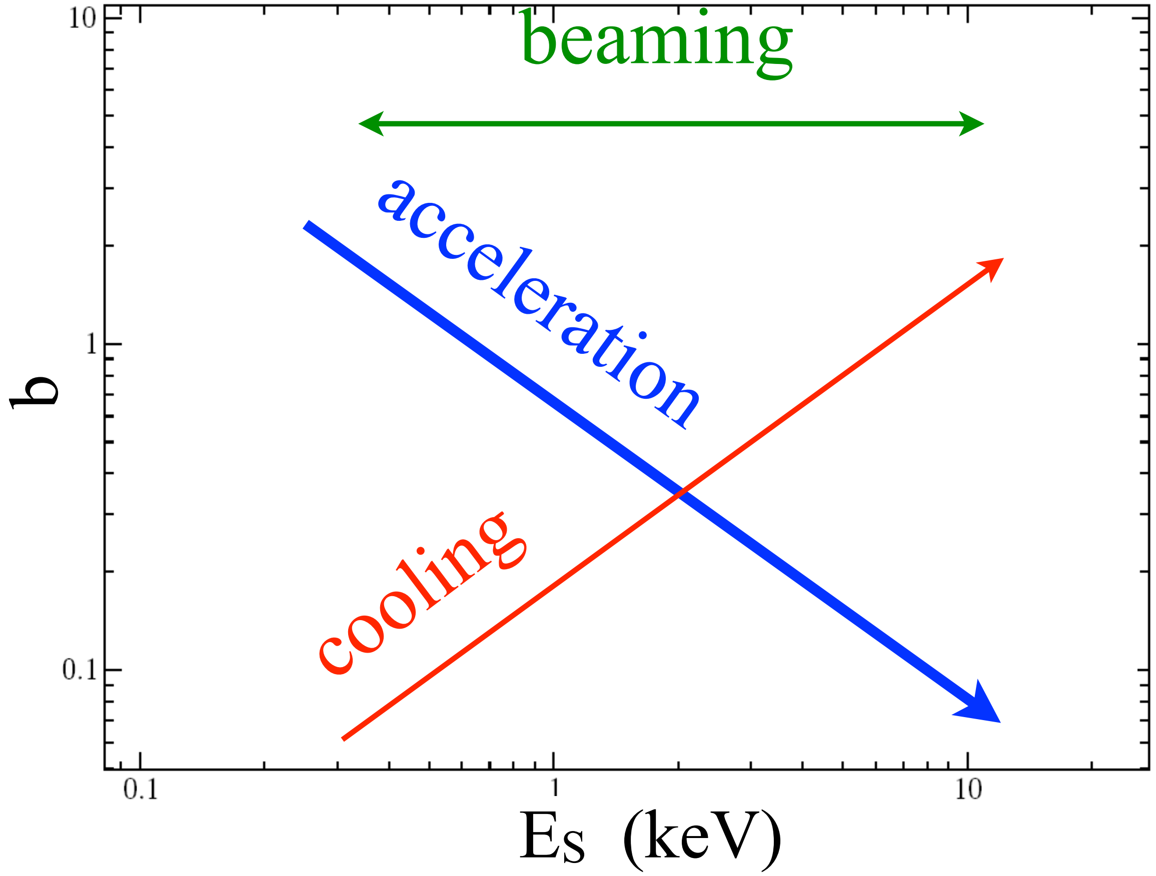

11 years of data:
PKS 0548-322,1H1426+418,
Mrk 501 ,1ES1959+650,
PKS2155-34

Long term Ep-vs-b trends hint for an acceleration dominated scenario

acceleration signature in the E_S-vs-L_s trend

long-trend main drivers

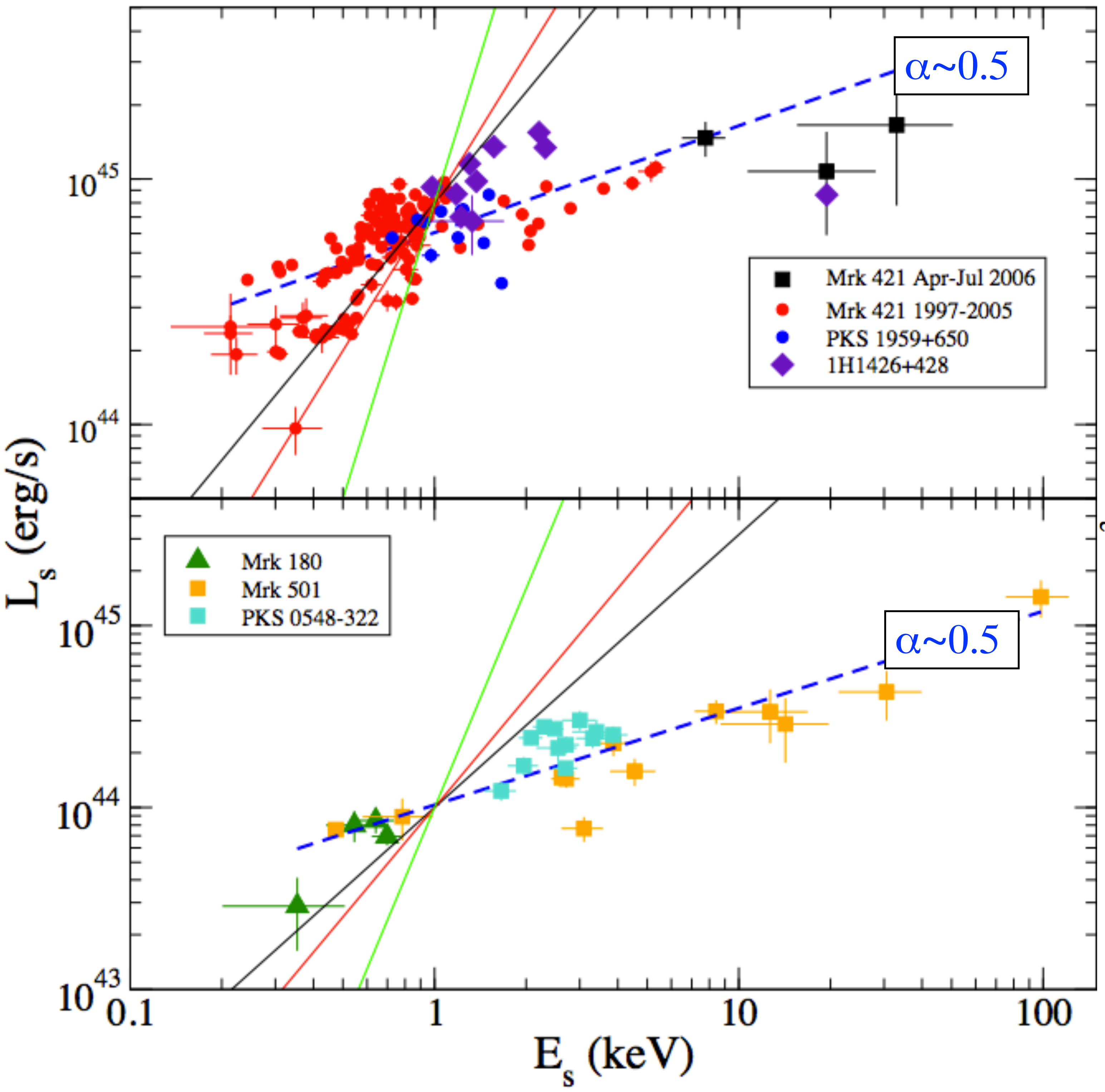

Tramacere A., et al.2009A&A...501

$$S_s(E_s) \propto n(\gamma_{3p})\gamma_{3p}^3 B^2 \delta^4$$

$$E_s \propto \gamma_{3p}^2 B\delta.$$

↓

$$S_s \propto (E_s)^\alpha$$

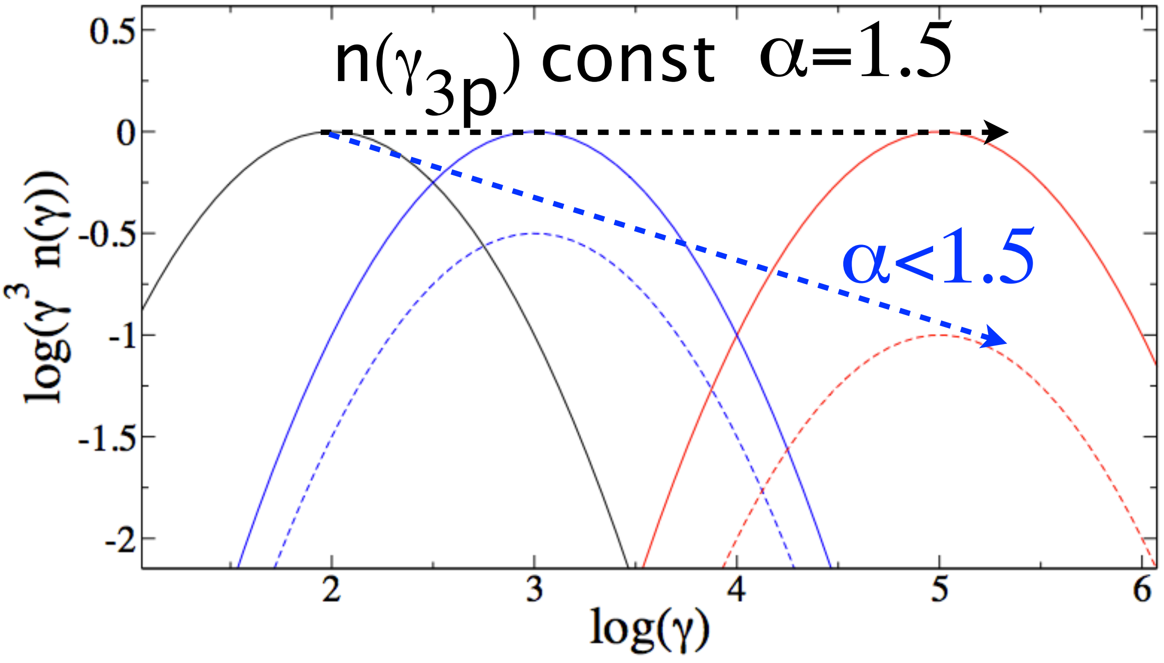

•γ_{3p}↑ and n(γ3p)↓ => α<1.5

acceleration+energy conservation

•B−>α=2.0,
•δ−>α=4

incompatible as long-trend main driver

The log-parabola origin:
physical insight

The origin of the log-parabolic shape: statistical derivation

fluctuation

$\varepsilon = \bar{\varepsilon} + \chi$

systematic

ε_i is a R.V.

$\gamma_{n_s} = \gamma_0 \Pi_{i=1}^{n_s} \varepsilon_i$

C.L. Theorem
multipl. case

log-normal distribution

Log-Parabolic representation

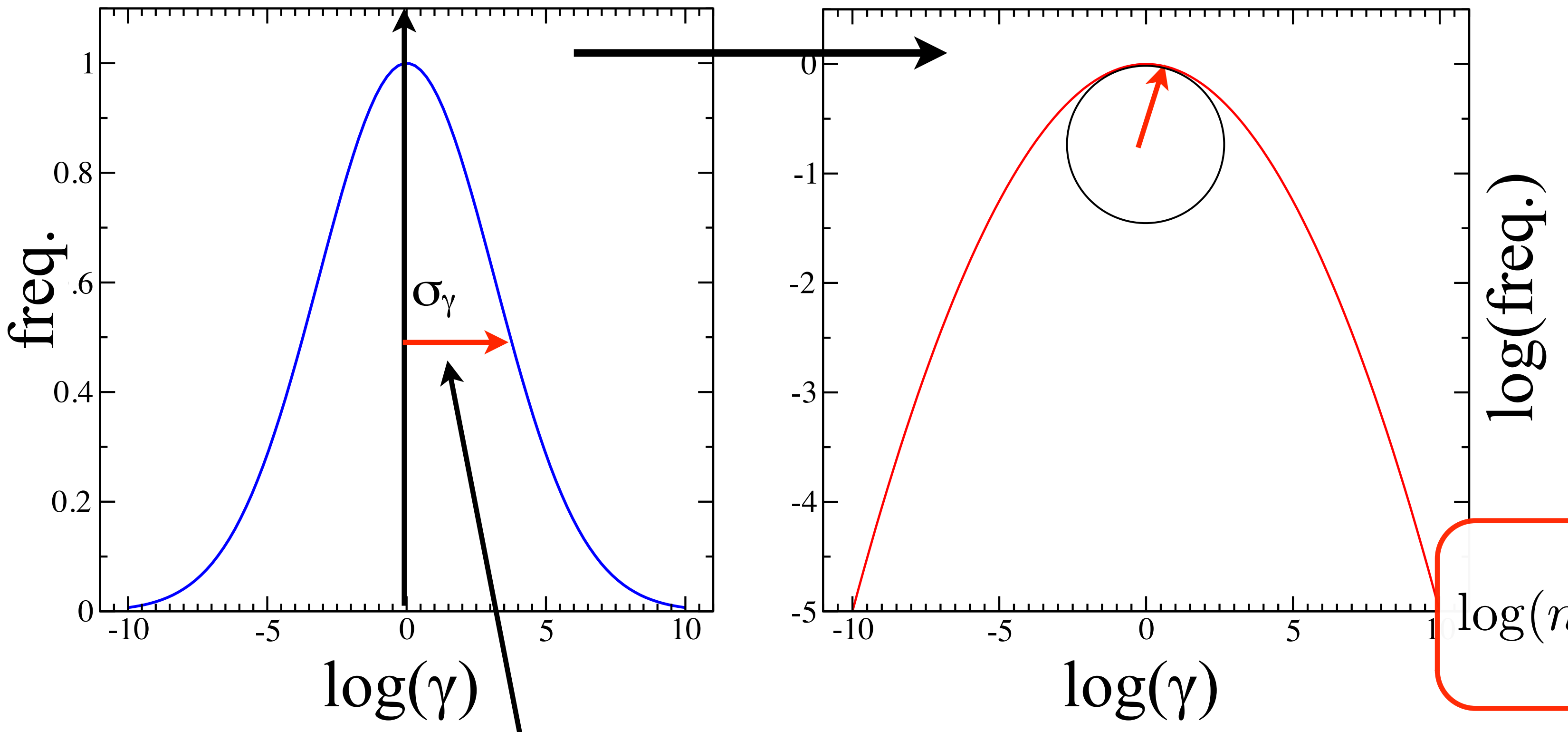

The curvature parameter *r* is inversely proportional to *n_s* and to σ^2_ε

$$\log(n(\gamma)) \propto \frac{(\log\gamma - \mu)^2}{2\sigma_\gamma^2} \propto r\;[\log(\gamma) - \mu]^2$$

$$\sigma_y^2 = \sigma^2(\log(\gamma)) \approx n_s\left(\frac{\sigma_\varepsilon}{\bar{\varepsilon}}\right)$$

curvature = $\frac{1}{\sigma_\gamma^2} = 2r$

$$r = \frac{c_e}{2n_s\left(\frac{\sigma_\varepsilon}{\bar{\varepsilon}}\right)^2}$$

The origin of the log-parabolic shape: diffusion equation approach

$$\frac{\partial n(\gamma,t)}{\partial t} = \frac{\partial}{\partial\gamma}\left\{-[S(\gamma,t)+D_A(\gamma,t)]n(\gamma,t)+D_p(\gamma,t)\frac{\partial n(\gamma,t)}{\partial\gamma}\right\} - \frac{n(\gamma,t)}{T_{esc}(\gamma)} + Q(\gamma,t)$$

$$\boxed{n(\gamma,t) = \frac{N_0}{\gamma\sqrt{4\pi D_{p0}t}}\exp\left\{-\frac{[\ln(\gamma/\gamma_0)-(A_{p0}-D_{p0})t]^2}{4D_{p0}t}\right\}}$$

analytical solution for:

$D_p \sim \gamma^q$, q=2

“hard-sphere” case

Melrose 1968, Kardashedv 1962

$$r \propto \frac{1}{D_{p0}t} \rightarrow D_{p0} \propto \left(\frac{\sigma_\varepsilon}{\bar{\varepsilon}}\right)^2$$

The curvature r is inversely proportional to ***t*=>*n_s*** and ***D_p*=>σ_ε**

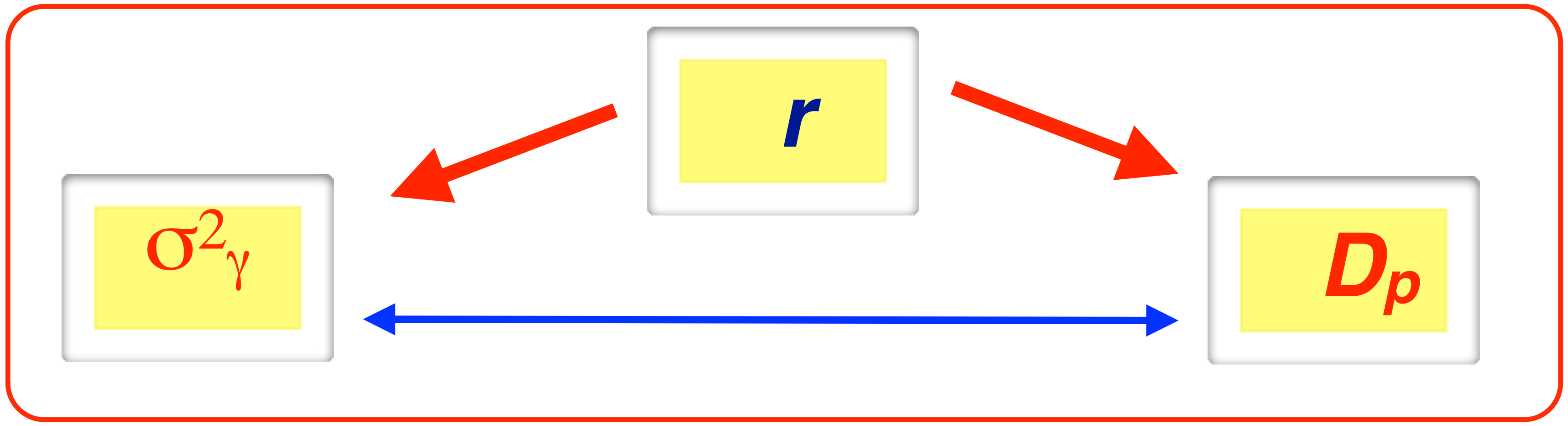

r

σ^2_γ

D_p

A self-consistent approach

self-consistent approach: **acc+cooling**

inj. term

$$L_{inj} = \frac{4}{3}\pi R^3 \int \gamma_{inj} m_e c^2 Q(\gamma_{inj}, t) d\gamma_{inj} \quad (erg/s)$$

systematic term

$$S(\gamma, t) \; = \; -C(\gamma, t) + A(\gamma, t)$$

cooling term $C(\gamma) = |\dot{\gamma}_{\mathrm{synch}}| + |\dot{\gamma}_{\mathrm{IC}}|$

syst. acc. term

$$A(\gamma) \quad = A_{p0}\gamma, t_A = \frac{1}{A_0}$$

Turbulent magnetic field ⟶ **momentum diffusion term**

$$W(k) = \frac{\delta B(k_0^2)}{8\pi}\left(\frac{k}{k_0}\right)^{-q}$$

$$t_D = \frac{p^2}{D_p} \approx \frac{< L > \beta_A^{-2}}{c}$$

set-up of the accelerator

- R~ 10^{13}-10^{15} cm
- δB/B<<1 , B~[0.01-1.0] G
- β_A ~ 0.1-0.5
- λ_{max}<R => ~ 10^{12} cm
- $\rho_g < \lambda_{max}$ => $\gamma_{max} \sim 10^{7.5}$

⟶ **t_D~10^4 s**

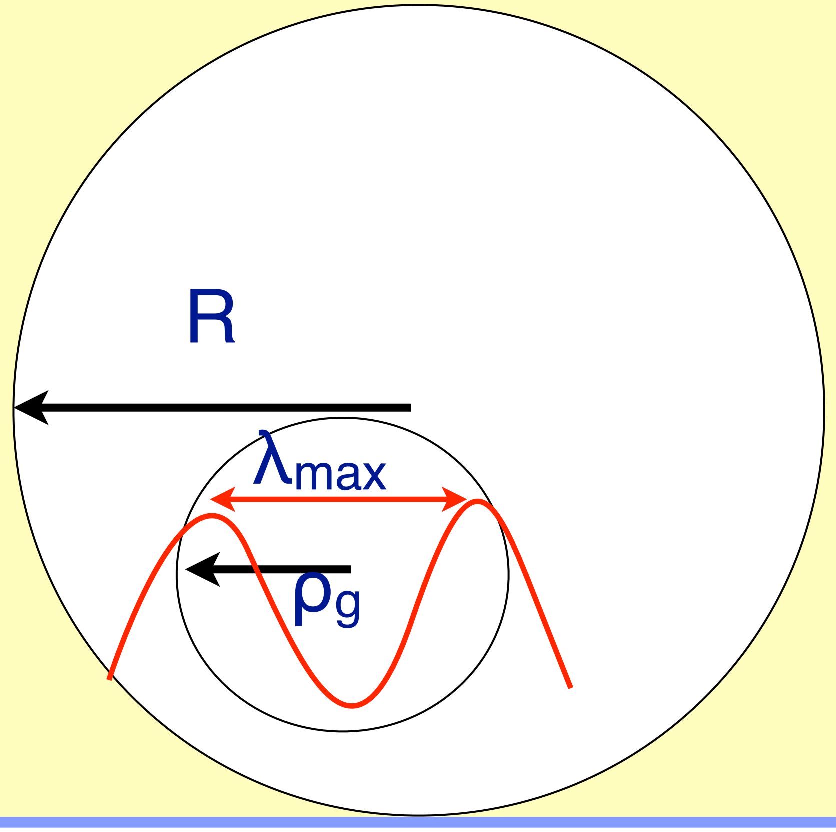

acc.-dominated-vs-equil.,R= 10^{15} cm, q=2

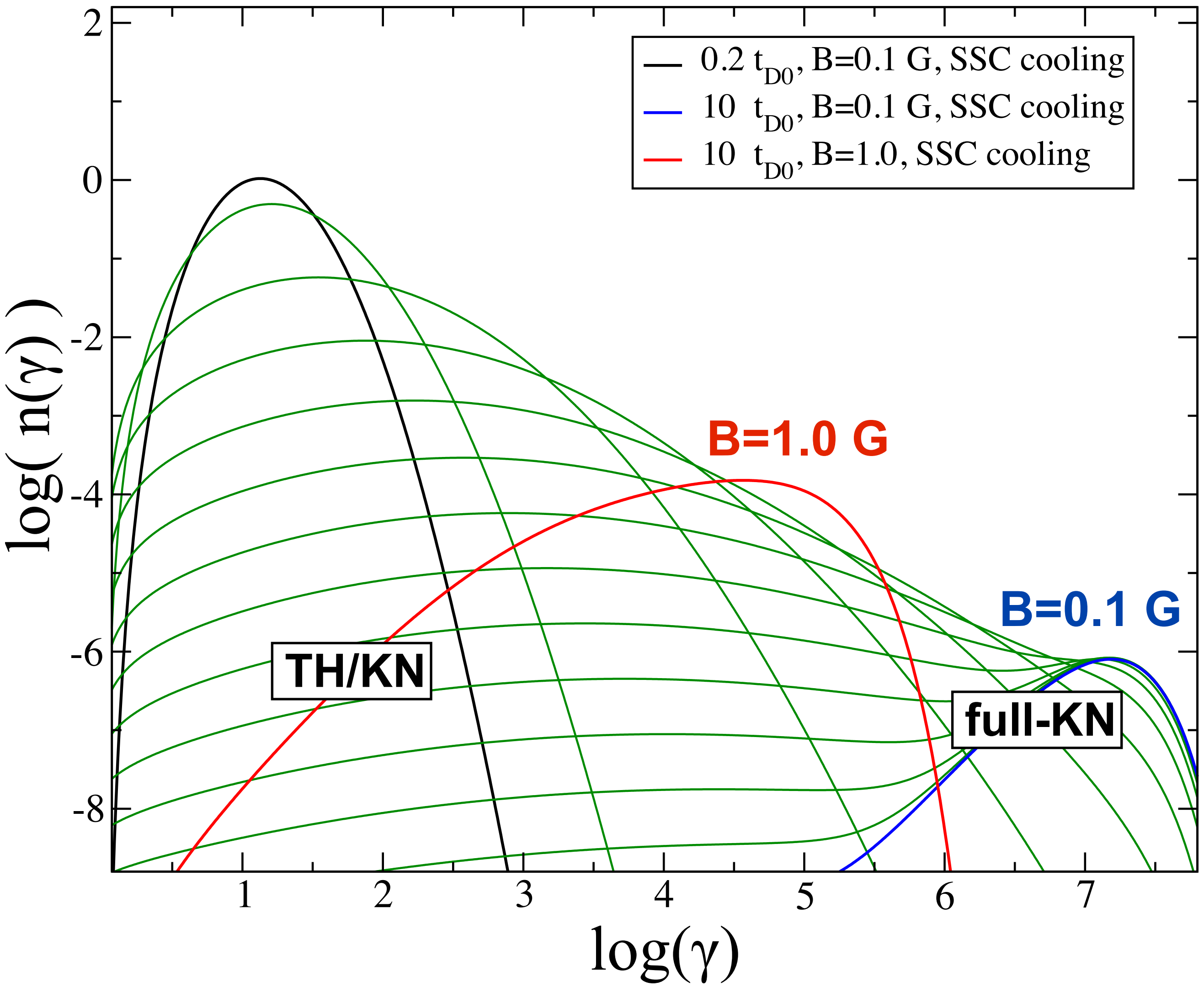

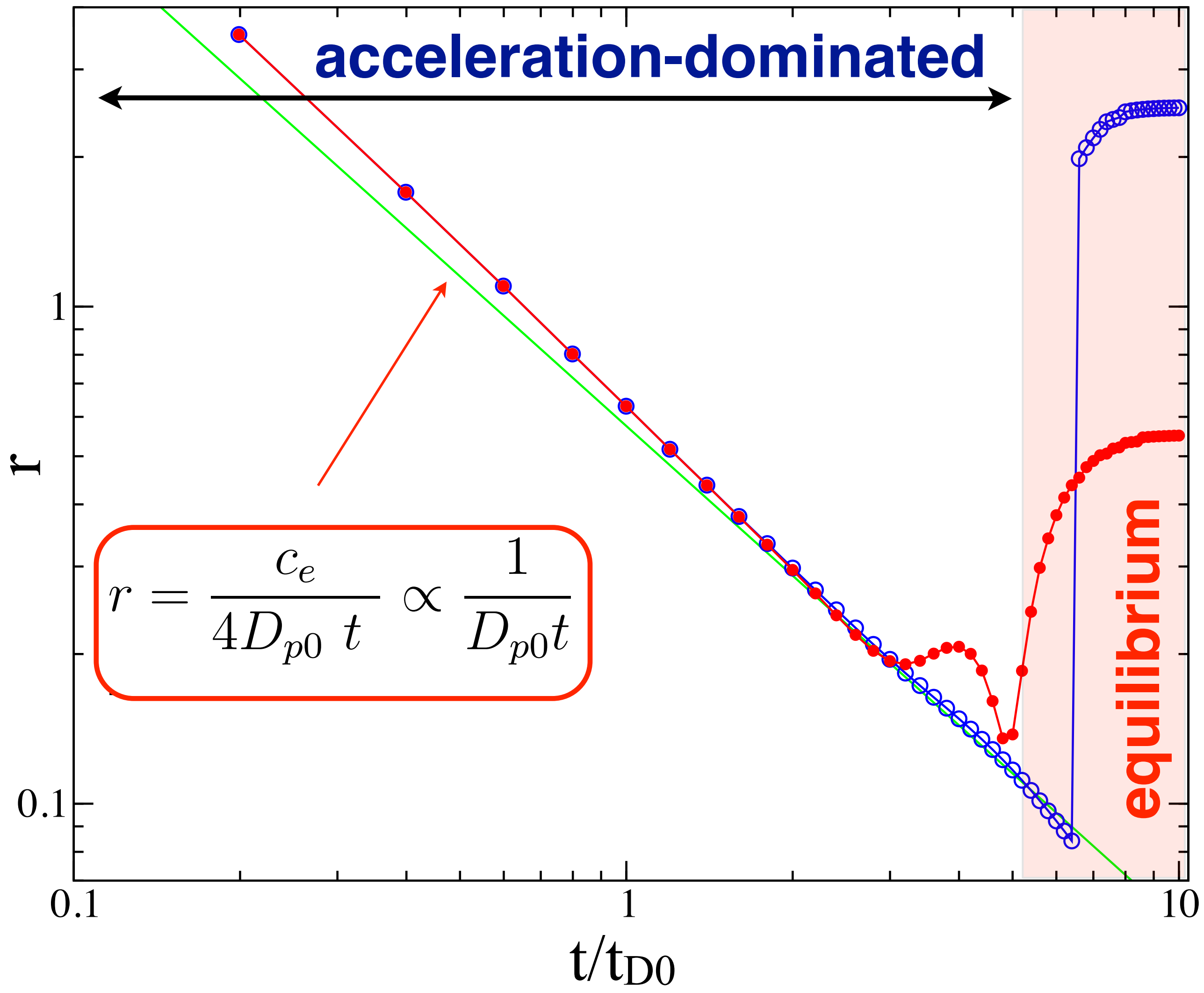

$$r = \frac{c_e}{4D_{p0}\ t} \propto \frac{1}{D_{p0}t}$$

- mono energetic inj., t_{inj}<<t_{acc}, t_{inj}<<t_{sim}
- we measure r@peak as a function of the time
- two phase: **acceleration-dominated**, **equilibrium**
- equil. distribution:
  - **f=1 for q=2 and S, full TH, or full KN**
- **equil. curv.: r~2.5, (r_{3p}~6.0) for TH or full KN**
- **equil. curv.: r~0.6, (r_{3p}~4.0) for TH-KN**

$$n(\gamma) \propto \gamma^2 \exp\left[\frac{-1}{f(q,\dot{\gamma})}\left(\frac{\gamma}{\gamma_{eq}}\right)^{f(q,\dot{\gamma})}\right]$$

D_p-driven trends $t_{D=}[1.5x10^4$-$1.5x10^5]$, L_{inj}=const.

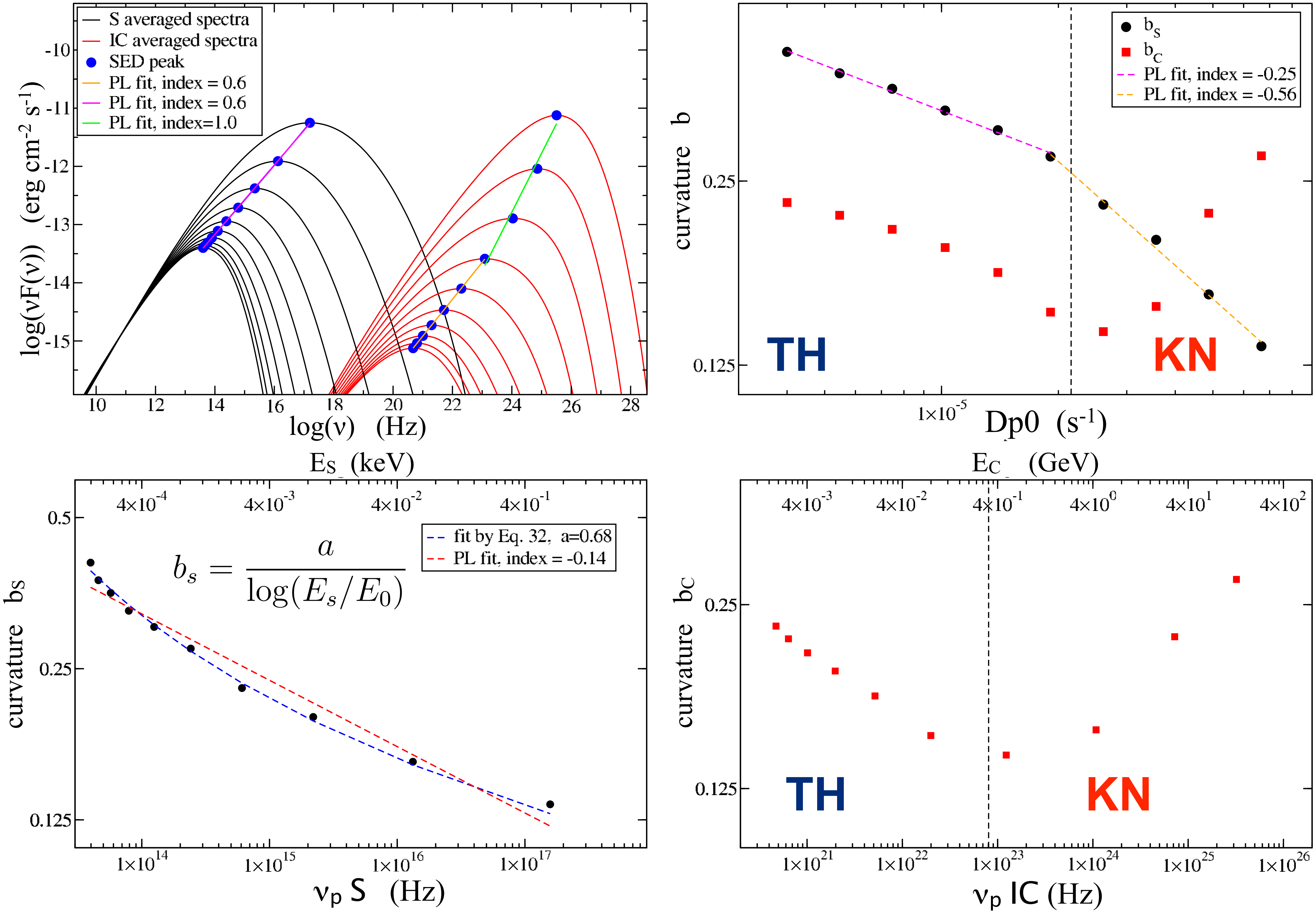

E_s-b_s X-ray trend and γ-ray predictions

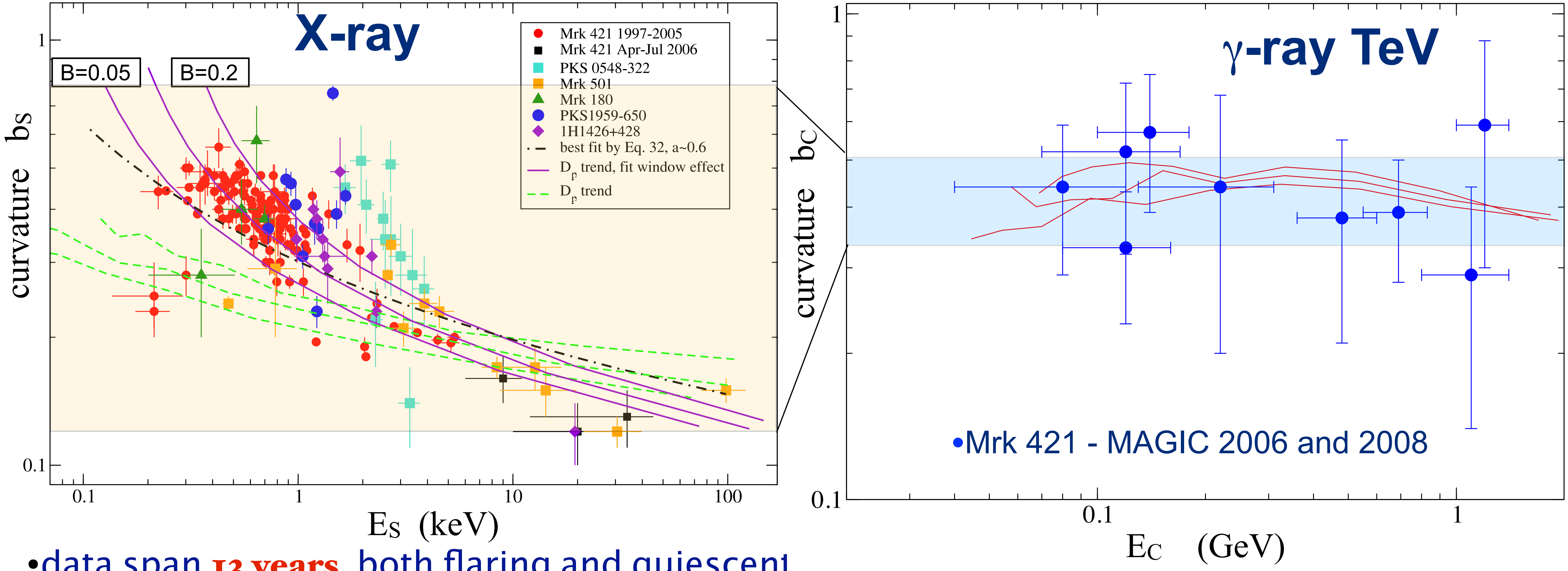

- data span **13 years**, both flaring and quiescent states
- We are able to reproduce these long-term behaviours, by changing the value of only one parameter (D_p)
- for q=2, curvature values imply distribution far from the equilibrium (b~1.2)
- More data needed at GeV/TeV, curvature seems to be cooling-dominated

$L_{\rm inj}$ (E_s–b_s trend)	(erg s^{-1})	5×10^{39}
$L_{\rm inj}$ (E_s–L_s trend)	(erg s^{-1})	5×10^{38}, 5×10^{39}
q		2
t_A	(s)	1.2×10^3
$t_{D_0} = 1/D_{P0}$	(s)	$[1.5 \times 10^4, 1.5 \times 10^5]$
$T_{\rm inj}$	(s)	10^4
$T_{\rm esc}$	(R/c)	2.0

E_s-L_s X-ray trend and γ-ray predictions

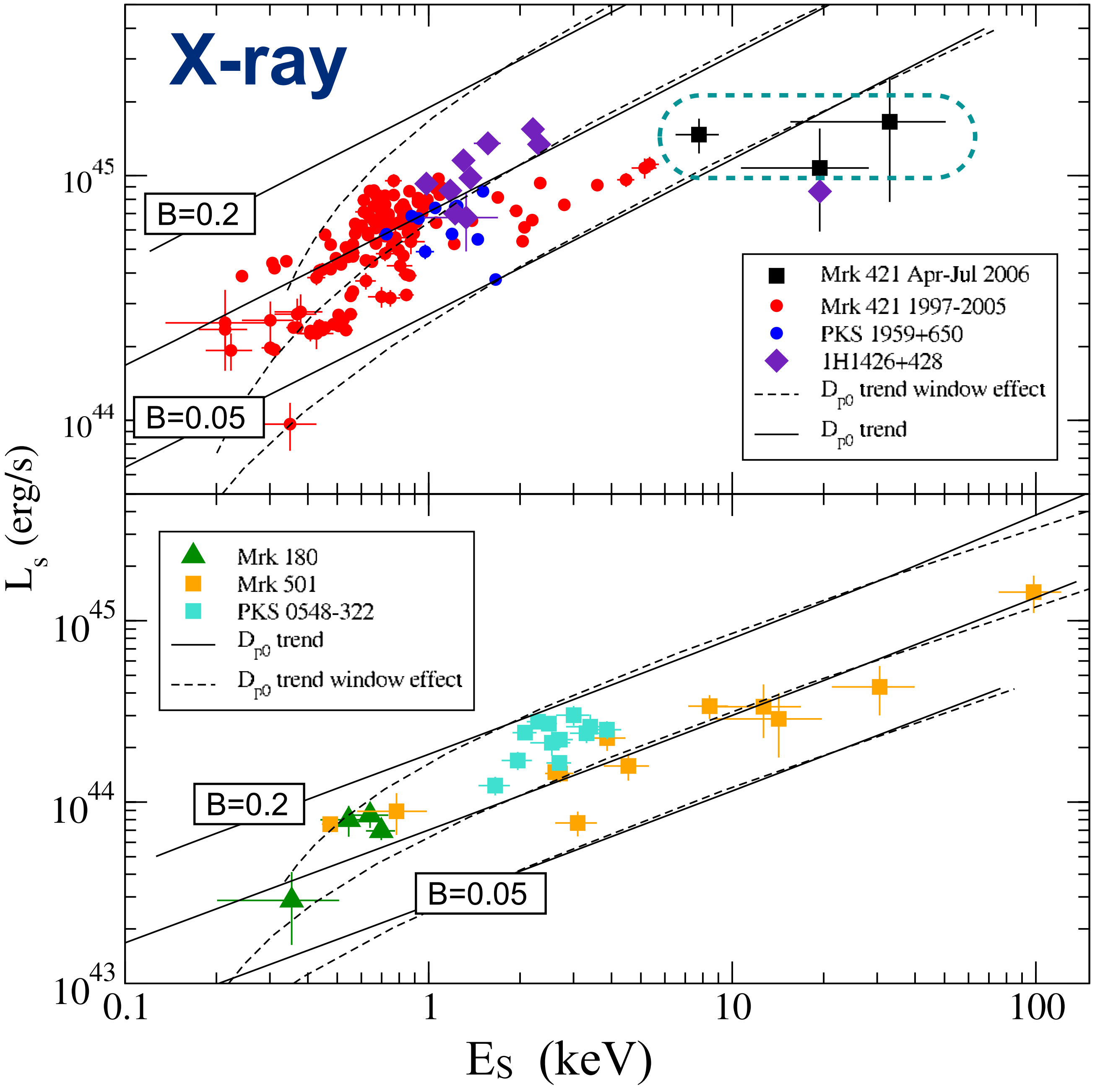

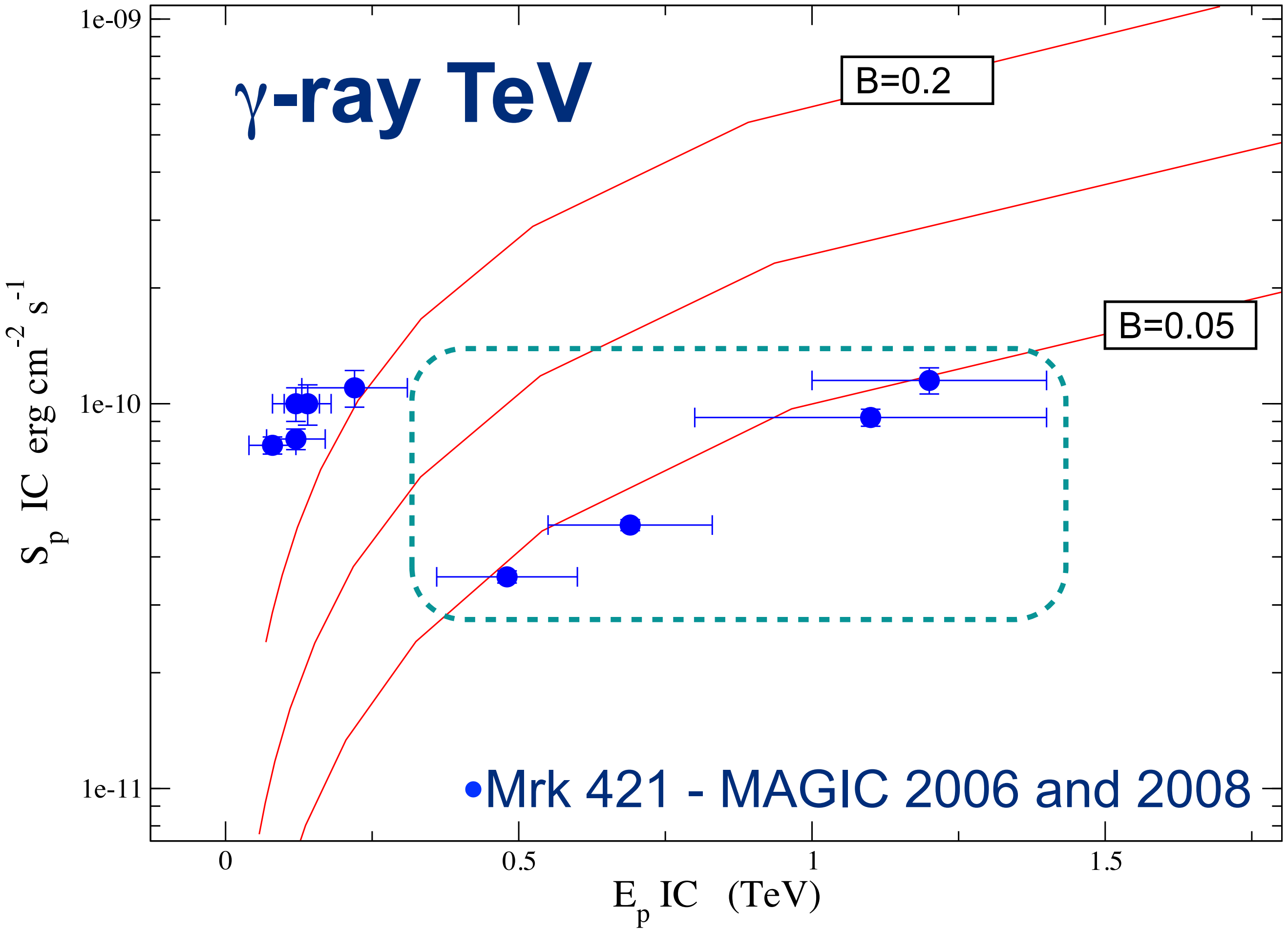

- the E_s–S_s (E_s–L_s) relation follows naturally from that between E_s and b_s
- the low L_{inj} objets (Mrk 501 vs Mrk 421) reach a larger E_S, compatibly with larger γ_{eq}
- Mrk 421 MGIC data on 2006 match very well the Synchrotron prediction with simultaneous X-ray data
- the average index of the trend $L_s \propto E_S^{\alpha}$ with α~0.6, is compatible with the data, and with a scenario in which a typical constant energy (L_{inj} xt_{inj}) is injected for any flare (jet-feeding problem), whilst the peak dynamic is ruled by the turbulence in the magnetic field.

Conclusions

- Log-parabola **is not a "*magic*" distribution, but it is not by chance, it has a physical interpretation compatible with a stochastic acceleration scenario, and, in this framework, the curvature parameter is an indicator of the momentum diffusion in the acceleration process**
- Log-parabolic distributions hint for an acceleration-dominated state, far from the equilibrium state, whilst at the equilibrium, maxwellian-like distribution are expected (TH/KN regime relevant to the equilibrium shape)
- Our stochastic scenario is able to reproduce the observed trends for a sample o 6 HBLs, spanning 13 years, with a small number of parameters. We found that the momentum diffusion can explain the Eb-vs-b trend, and that the Lp-vs-Ep trends follows from it naturally, provided that a constant typical energy ($L_{inj}xt_{inj}$) is injected.
- The crosscheck with γ-ray data, is mandatory to constrain better the parameter space of the cooling and acceleration scenario (and to break some of the degeneracy among the parameters). We predict GeV/TeV trends, basing on the X-ray data, and we find a reasonable agreement with the literature data, but a larger amount of γ-ray data is needed
- Future instrument (γ-ray/X-ray), thanks to larger statistics, will provide tighter constraints possible to the measure of the curvature variation, and to discriminate between log-par and exp. cut-off, with an higher accuracy, allowing to discriminate between acceleration and cooling dominated trends.

online SSC/EC tool @ http://isdc-web00.isdc.unige.ch/sedtool/

SSC/EC Simulator
author: andrea.tramacere@unige.ch

- Model Menu

Jet

1e+16 R (cm)
0.12 B (G)
0.03 z (red shift)
13.0 Γ (Bulk Lorentz Factor)
1.0 θ (viewing angle)

n(γ)

60.0 N
1.0 γ_min
100000000.0 γ_max
log-par+pl elec distr
0.7 r
1.6 s
8500.0 γ_0

emission scenario

Yes Synch
Yes IC
NO EC

☐ save model

SED tool output : Test version

Backup slides

MRK 421 SWIFT XRT obs. on 29/04/05

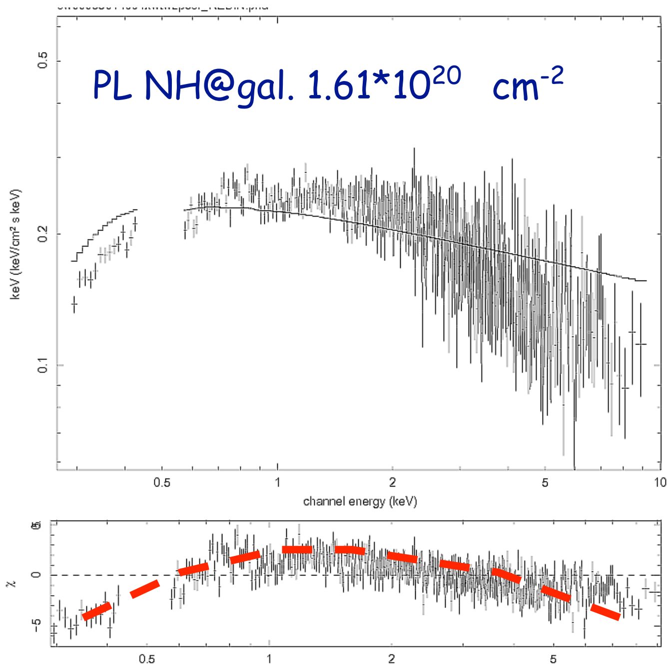
PL NH@gal. $1.61*10^{20}$ cm^{-2}

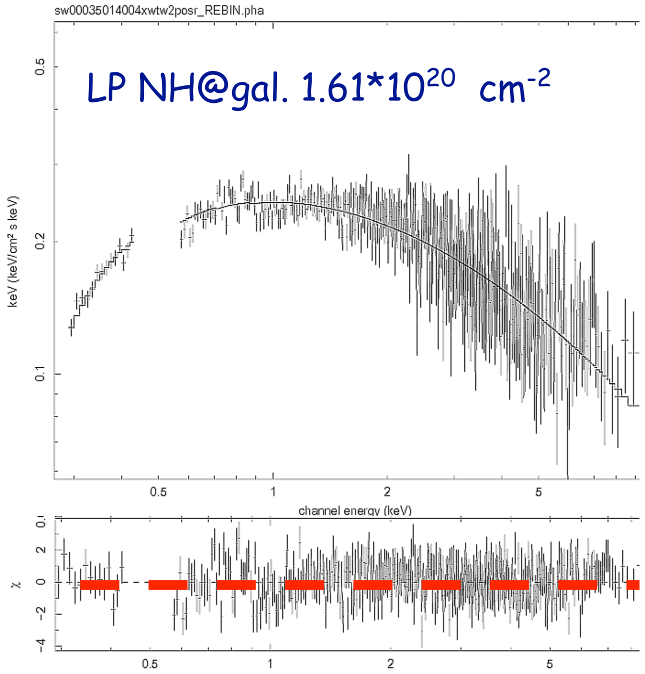
LP NH@gal. $1.61*10^{20}$ cm^{-2}

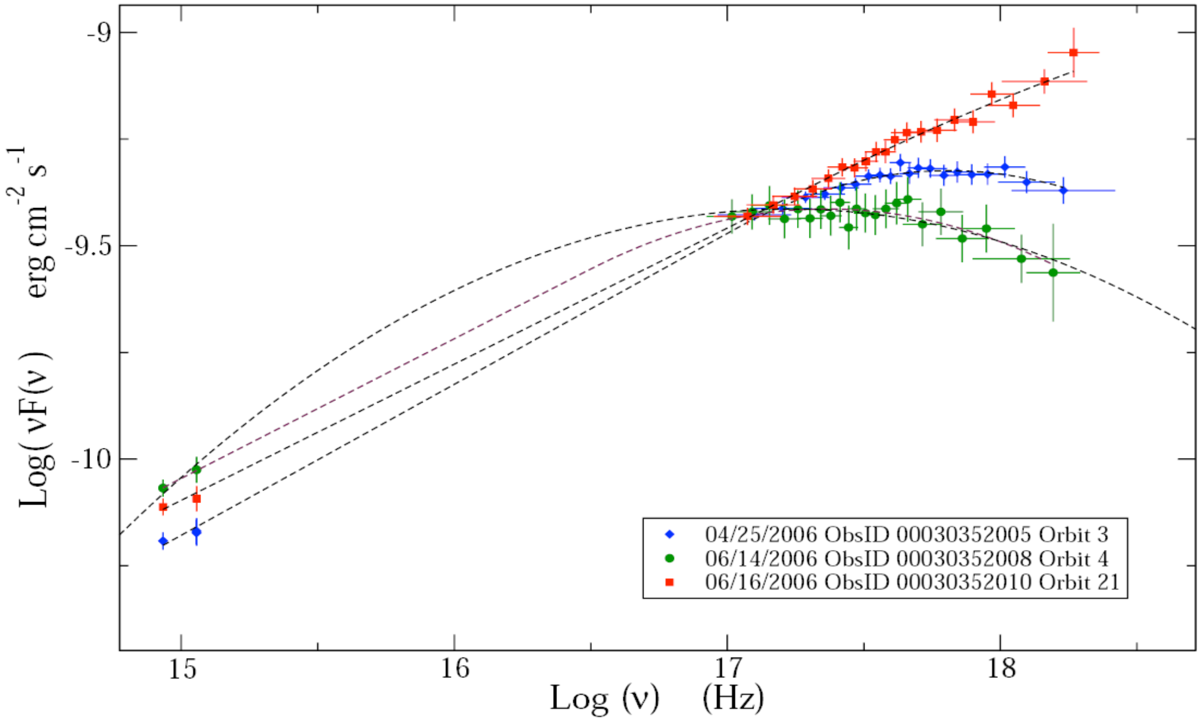

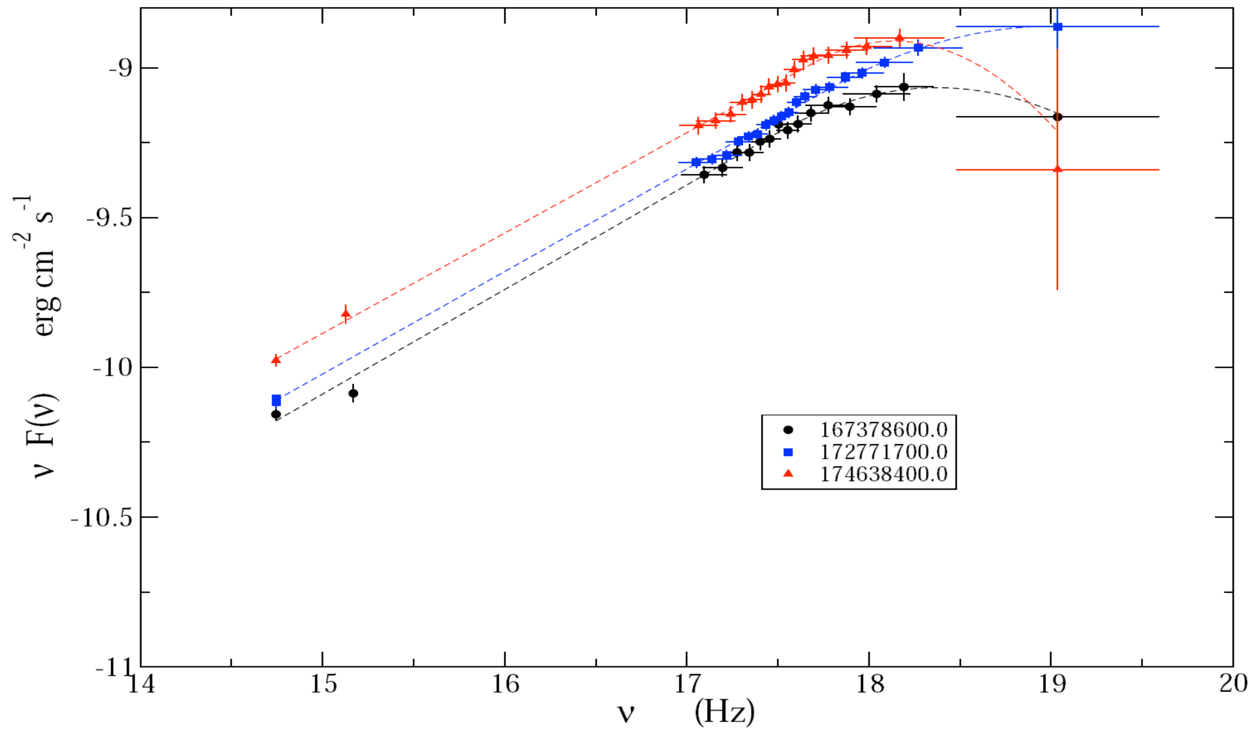

Relation between the observed synchrotron curvature (b) and that of the emitting electrons (r)

$$n(\gamma) = K\,(\gamma/\gamma_c)^{-s}, \qquad \gamma \le \gamma_c$$
$$n(\gamma) = K\,(\gamma/\gamma_c)^{-(s+r\ \mathrm{Log}(\gamma/\gamma_c))}, \gamma > \gamma_c$$

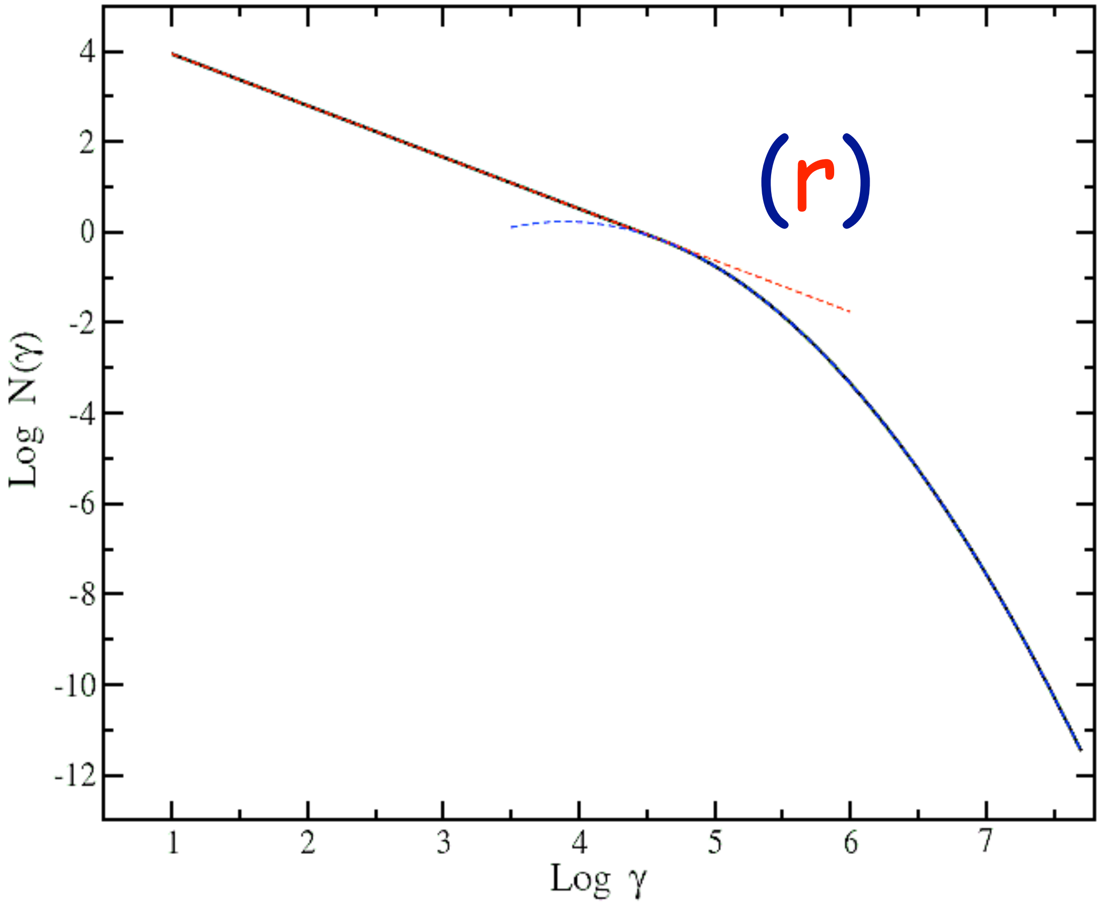

$$F(E) = K\ E^{-(a+b\ \log(E))}$$

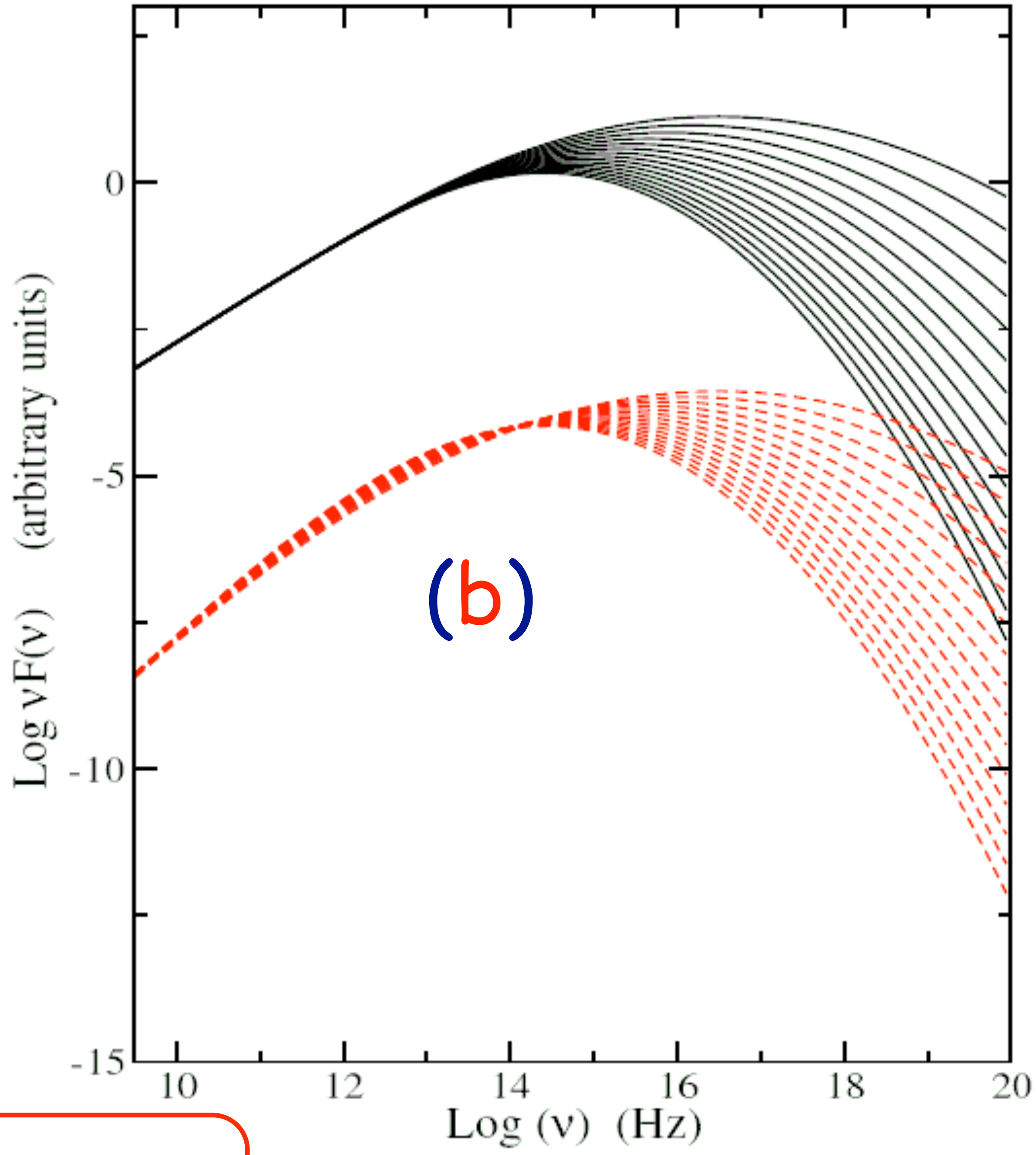

Accurate numerical computation b~r/5 @ 10 %

A test for Homogeneous SSC Model

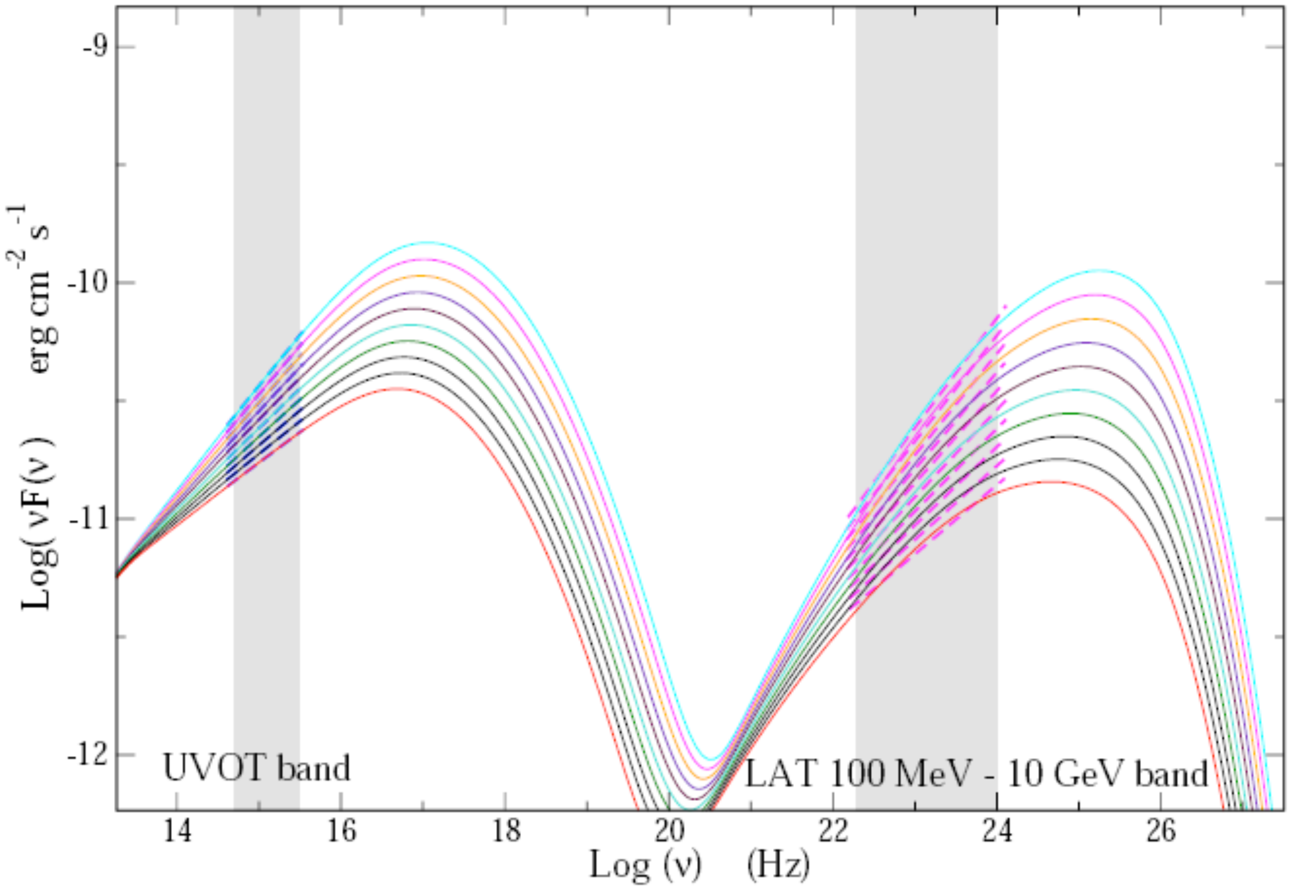

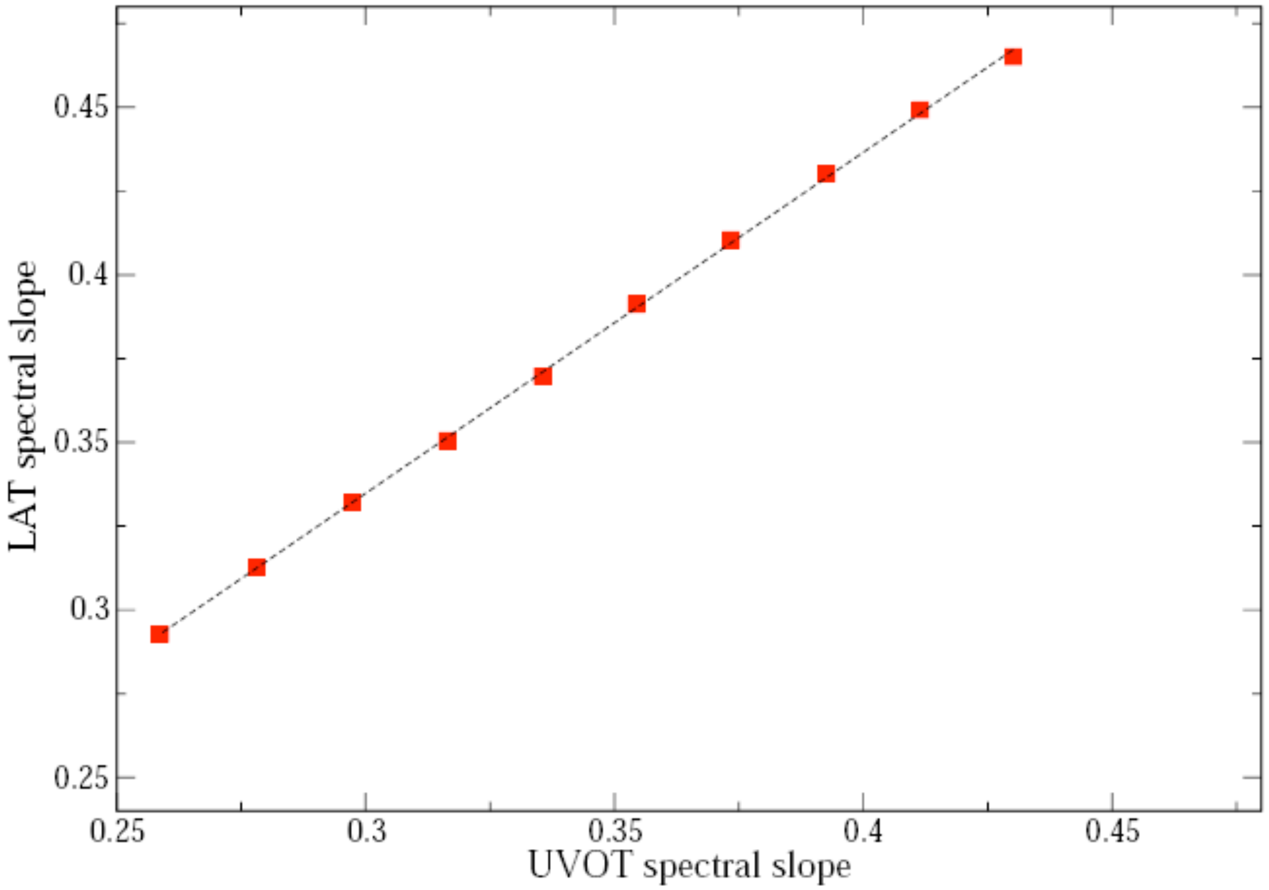

Due to the K-N effect, TeV IC photons are most efficiently produced by e^- emitting @ E>~1keV and up-scattering UV-to-soft-X-ray photons, and GeV photons are efficiently produced by e^- radiating @ E~<1keV and up-scattering UV-to-soft-X-ray photons. Moreover UV photons are much more numerous than X-ray ones.

We expect a strong correlation between the Swift/UVOT and Fermi-LAT spectral index.

IC intrinsic curvature and TeV emission

Massaro E.,Tramacere A. et al. A&A 2006

fixed $\gamma_0=10^3, 2*10^4$

change r and and the center of the range over which the IC curvature is measured

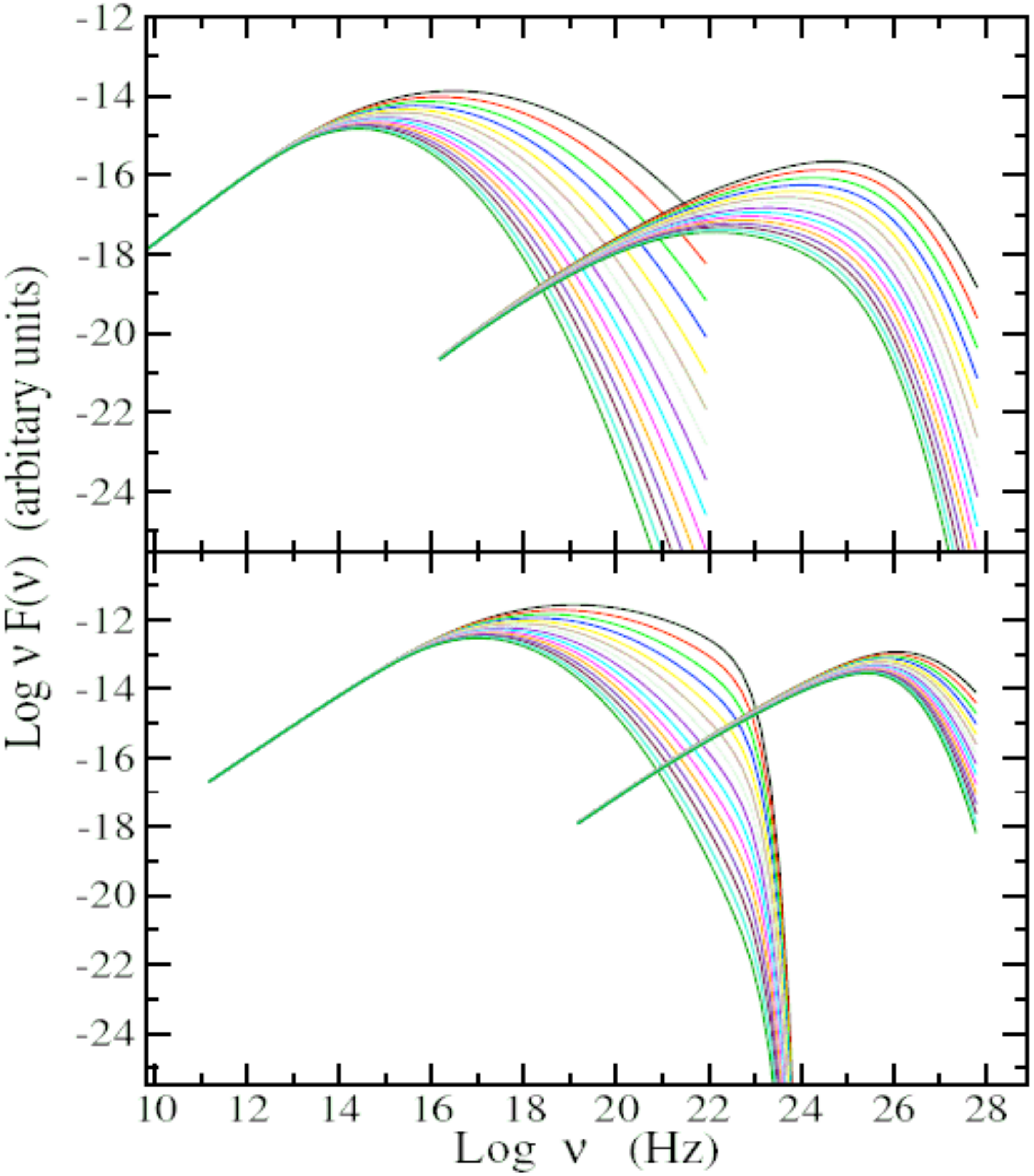

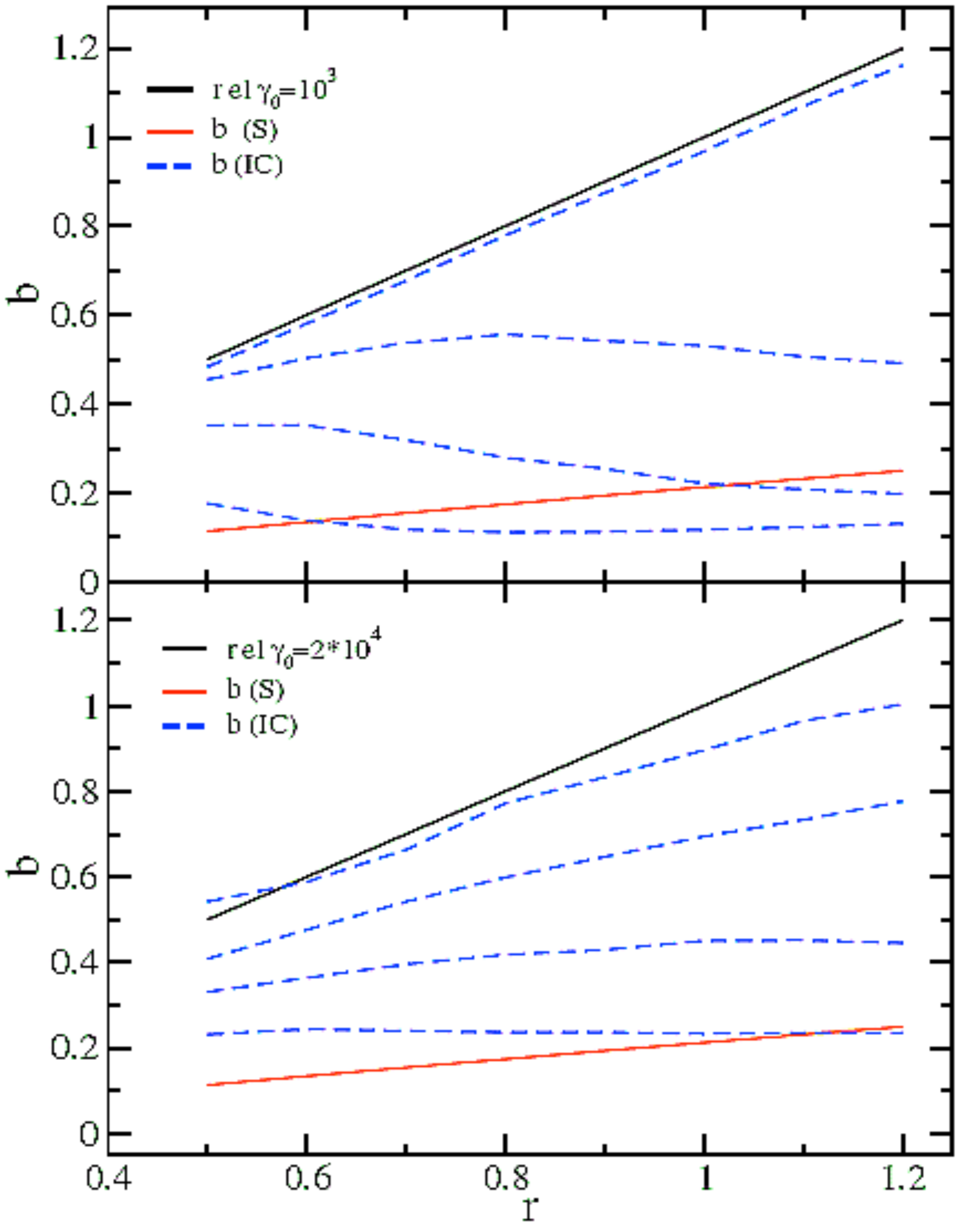

Cut-off interpretation as due only to the interaction among EBL and TeV photons

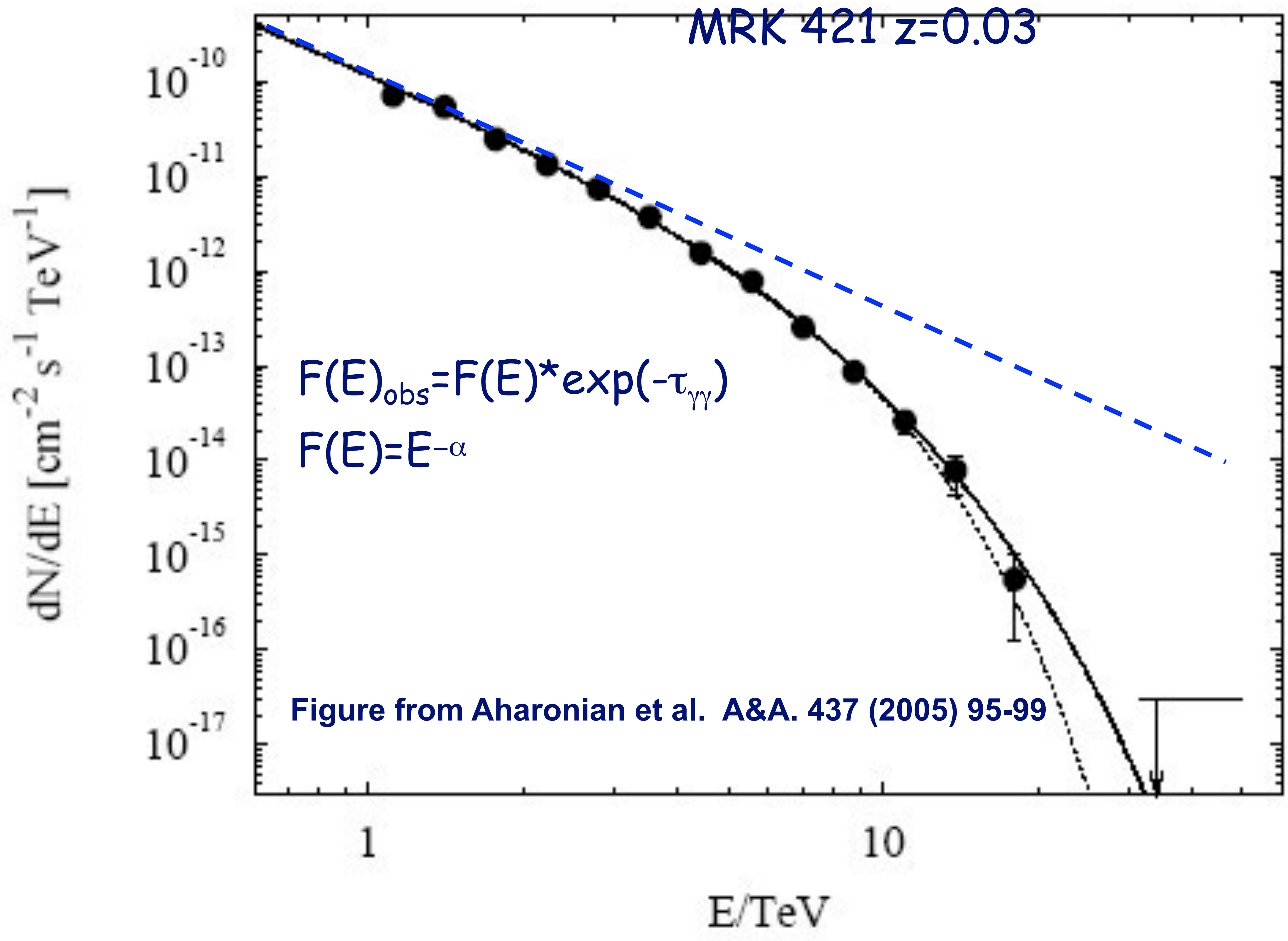

Figure from Aharonian et al. A&A. 437 (2005) 95-99

HBL Mrk 501 1997 large Flare

Massaro E., Tramacere A.,et al. A&A 2006

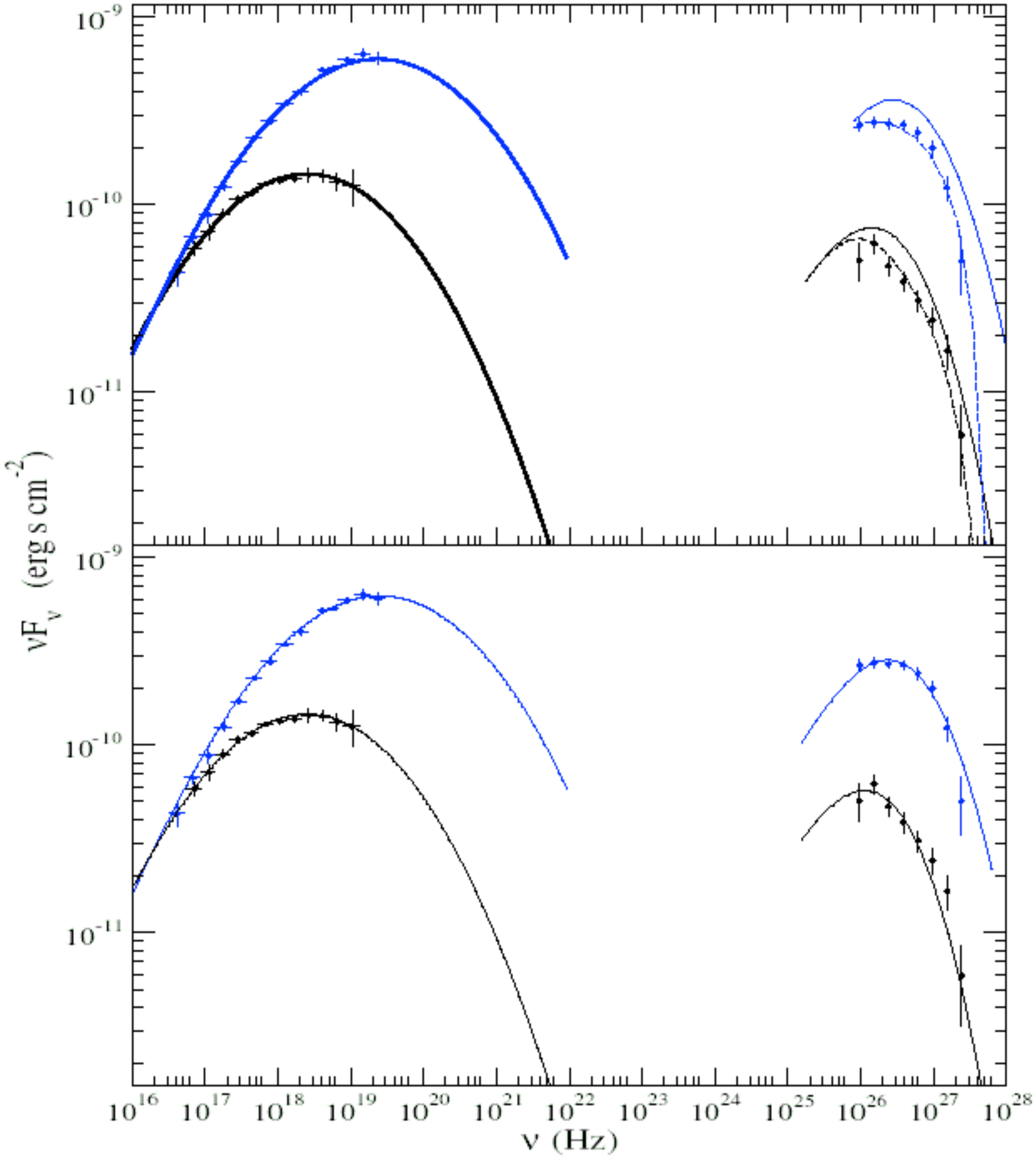

- We used the lowest EBL realization from Dwek and Krennrich 2005, to evaluate EBL attenuation for Mrk 501

- Within a One-Zone SSC scenario, our model requires low EBL densities to explain cut-off and curvature in the TeV spectra of blazars

TeV detection of High z TeV BLAZARS is in agreement with our model.

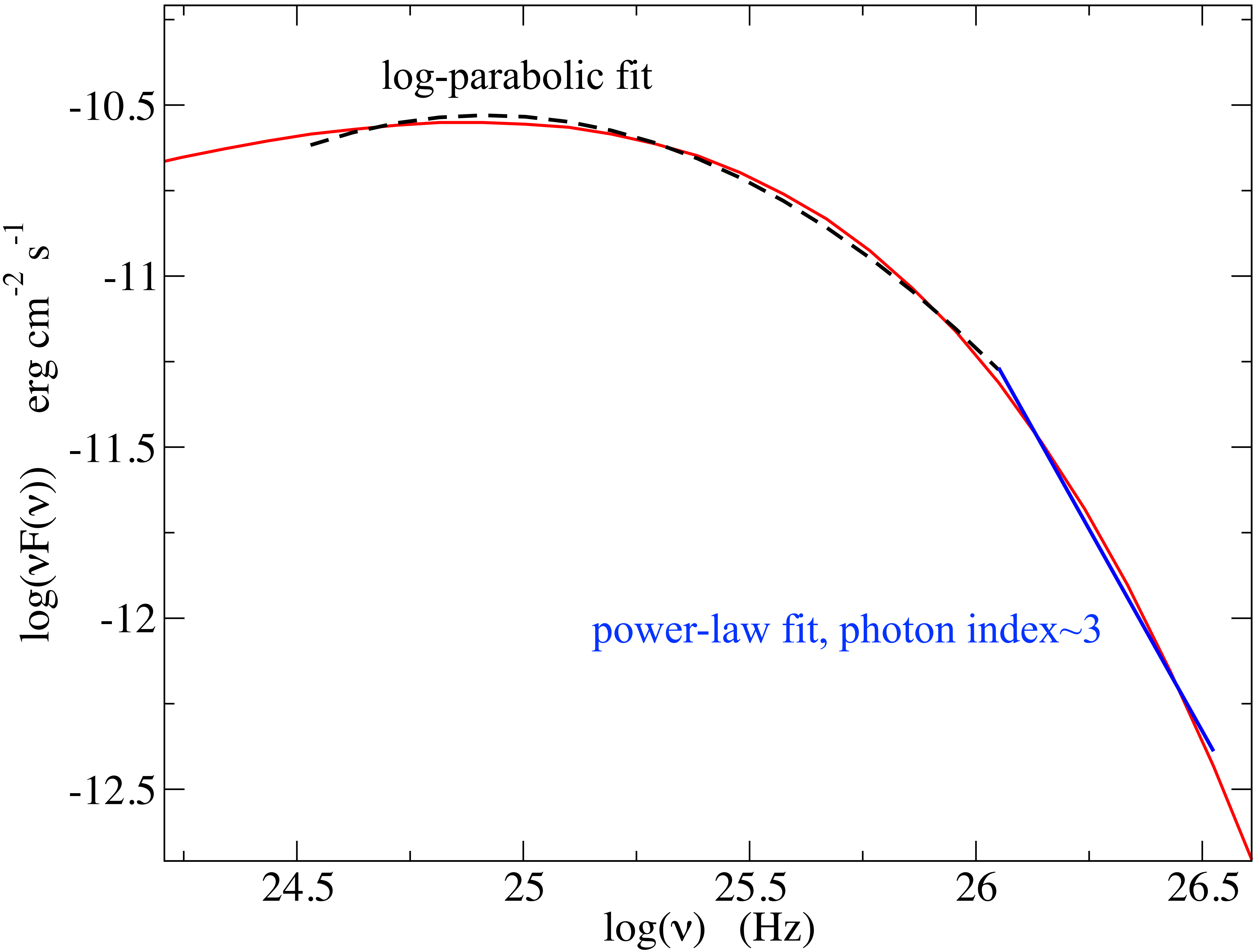
log-parabolic fit
power-law fit, photon index~3
-10.5
-11
-11.5
-12
-12.5
24.5
25
25.5
26
26.5
log(νF(ν)) erg cm^{-2} s^{-1}
log(ν) (Hz)

The origin of the log-parabolic shape: statistical approach

$$\gamma_{n_s} = \varepsilon_{n_s}\gamma_{n_s-1} = \gamma_{n_s-1}(1 + \Delta\gamma_{n_s-1}/\gamma_{n_s-1})$$

particle energy at step *n*$_s$

$$\varepsilon = \bar{\varepsilon} + \chi$$

energy gain = syst.+ fluctuation

systematic gain

is a RV with mean=0, and variance σ_χ^2,

$$\gamma_{n_s} = \gamma_0 \Pi_{i=1}^{n_s} \varepsilon_i$$

This equation clearly shows that the final energy distribution (n(γ) = dN(γ)/dγ) will result from the product of the random variables *ε*$_i$.

$$n(\gamma) = \frac{N_0}{\gamma\sigma_\gamma\sqrt(2\pi)} \exp\left[-(\ln\ \gamma - \mu)^2/2\sigma_\gamma^2\right]$$

$$\mu = \langle \ln\ \gamma \rangle,\ \sigma_\gamma^2 = \sigma^2(\ln\ \gamma)$$

C.L. Theorem
multiplicative case
log-normal distribution

we can determine $\mu = \langle \ln \gamma \rangle$, $\sigma_\gamma = \sigma (\ln \gamma)$ by expanding

$$\ln\ \gamma_{n_s} = \ln\ \gamma_0 + \Sigma_{i=1}^{n_s} \ln\ (\bar{\varepsilon} + \chi_i)$$

$$\mu = \ln\ (\gamma_0) + n_s \left[\ln\ \bar{\varepsilon} - \frac{1}{2} \left(\frac{\sigma_\varepsilon}{\bar{\varepsilon}} \right)^2 \right]$$

$$\sigma_\gamma^2 \approx n_s \left(\frac{\sigma_\varepsilon}{\bar{\varepsilon}} \right)^2$$

Log-Parabolic distribution

$$\log n(\gamma) = K - \log \gamma - \frac{\left(c_e \log \frac{\gamma}{\gamma_0} - n_s \left[c_e \log\ \bar{\varepsilon} + \left(\frac{\sigma_\varepsilon}{2\bar{\varepsilon}} \right)^2 \right] \right)^2}{c_e 2 n_s \left(\frac{\sigma_\varepsilon}{\bar{\varepsilon}} \right)^2}$$

$$r = \frac{c_e}{2 n_s \left(\frac{\sigma_\varepsilon}{\bar{\varepsilon}} \right)^2}$$

The curvature *r* is inversely proportional to *n_s* and to σ_ε

The origin of the log-parabolic shape: the Diffusion equation approach

$$\frac{\partial n(\gamma,t)}{\partial t} = \frac{\partial}{\partial\gamma}\left\{ - [S(\gamma,t) + D_A(\gamma,t)]n(\gamma,t) + D_p(\gamma,t)\frac{\partial n(\gamma,t)}{\partial\gamma}\right\} - \frac{n(\gamma,t)}{T_{esc}(\gamma)} + Q(\gamma,t)$$

$$W(k) = \frac{\delta B(k)^2}{8\pi} = \frac{\delta B(k_0)^2}{8\pi}\left(\frac{k}{k_0}\right)^{-q}$$

Turbulent magnetic field

$$D_p \approx \beta_A^2\left(\frac{\delta B}{B_0}\right)^2\left(\frac{\rho_g}{\lambda_{max}}\right)^{q-1}\frac{p^2c^2}{\rho_g c}$$

momentum diffusion coeff. (part-wave acc.)

$$\boxed{n(\gamma,t) = \frac{N_0}{\gamma\sqrt{4\pi D_{p0}t}}\exp\left\{ - \frac{[\ln(\gamma/\gamma_0) - (A_{p0} - D_{p0})t]^2}{4D_{p0}t}\right\}}$$

analytical solution for q=2
“hard-sphere” case

$$r = \frac{c_e}{4D_{p0}\ t} \propto \frac{1}{D_{p0}t} \longrightarrow D_{p0} \propto \left(\frac{\sigma_\varepsilon}{\bar{\varepsilon}}\right)^2$$

The curvature *r* is inversely proportional to ***t=>n_s*** and ***D_p=>σ_ε***

Numerical Self Consistent Approach

- both analytical and statistical approaches explain the link r–D–t r–σ–n_s
- but ignore the radiative contribution, and competition between radiative and accelerative time scales
- we solve numerically the continuity equation in order to have a self-consistent description of the problem

$$\frac{\partial n(\gamma,t)}{\partial t} = \frac{\partial}{\partial\gamma}\left\{ -[S(\gamma,t) + D_A(\gamma,t)]n(\gamma,t) + D_p(\gamma,t)\frac{\partial n(\gamma,t)}{\partial\gamma}\right\} - \frac{n(\gamma,t)}{T_{esc}(\gamma)} + Q(\gamma,t)$$

$$\begin{aligned}
\dot\gamma_{synch} &= \frac{4\sigma_T c}{3m_e c^2}\gamma^2 U_B = C_0\gamma^2 U_B \\
\dot\gamma_{IC} &= \frac{4\sigma_T c}{3m_e c^2}\gamma^2 \int f_{KN}(4\gamma\epsilon_0)\epsilon_0 n_{ph}(\epsilon_0)d\epsilon_0 = C_0\gamma^2 F_{KN}(\gamma) \\
C(\gamma) &= \dot\gamma_{synch} + \dot\gamma_{IC} = C_0\gamma^2(U_B + F_{KN}(\gamma))
\end{aligned}$$

$$\begin{cases}
D_p(\gamma) = D_{p0}\left(\frac{\gamma}{\gamma_0}\right)^q, & t_D = \frac{1}{D_{p0}}\left(\frac{\gamma}{\gamma_0}\right)^{2-q} \\
D_A(\gamma) = 2D_{p0}\left(\frac{\gamma}{\gamma_0}\right)^{q-1}, & t_{DA} = \frac{1}{2D_{p0}}\left(\frac{\gamma}{\gamma_0}\right)^{2-q} \\
A(\gamma) = A_{p0}\gamma, & t_A = \frac{1}{A_0}
\end{cases}$$

$$L_{inj} = \frac{4}{3}\pi R^3 \int \gamma_{inj} m_e c^2 Q(\gamma_{inj},t)d\gamma_{inj} \quad (erg/s)$$

Physical set-up (R,δ,B,q)

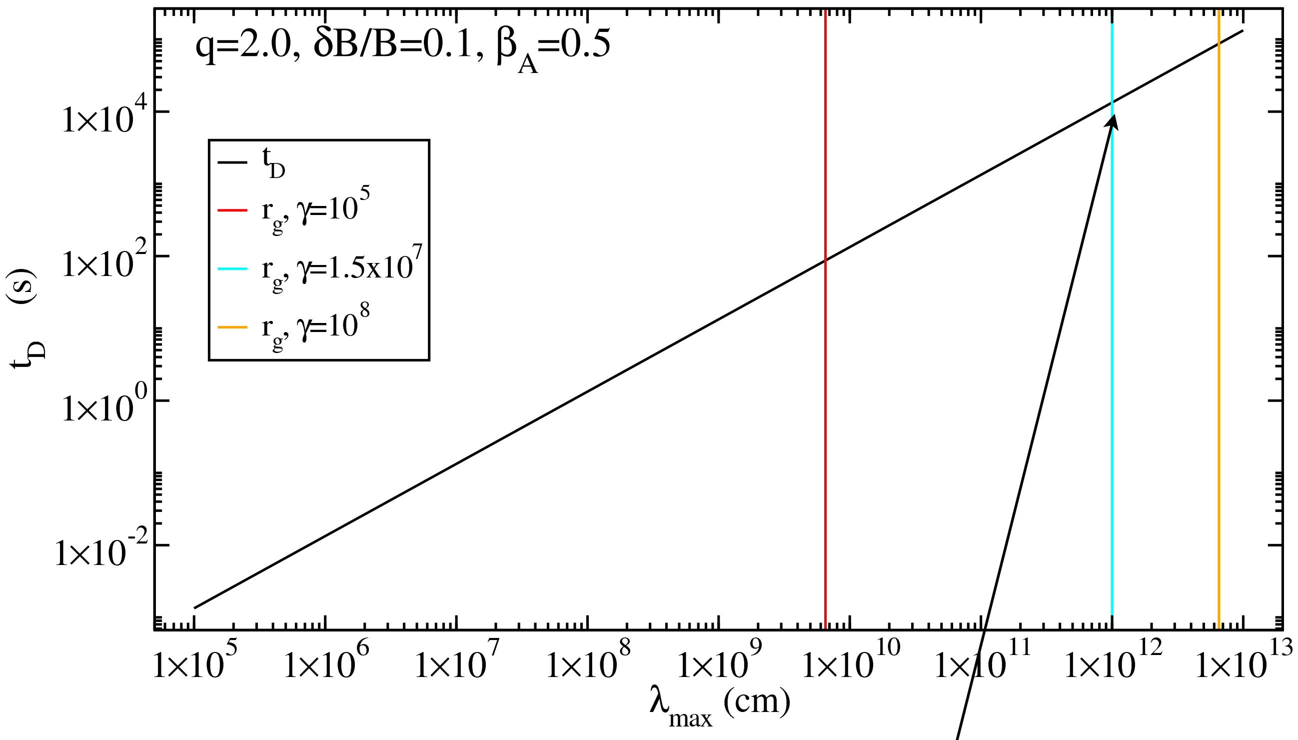

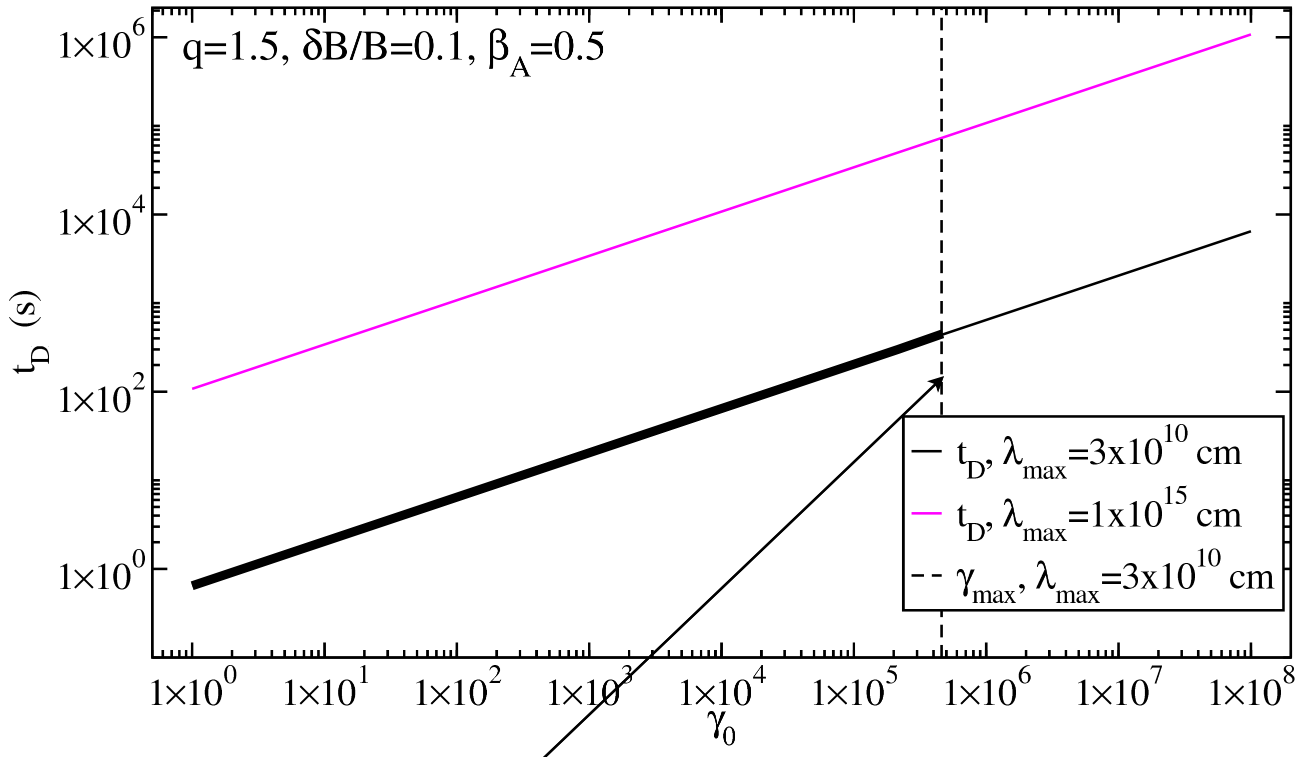

$\rho_g<\lambda_{max}$

- R~ 10^{13}-10^{15} cm
- δB/B<<1 , B~[0.01-0.1] G
- β_A ~ 0.1-0.5
- λ_{max}<R => ~ 10^{12} cm
- $\rho_g<\lambda_{max}$ => γ_{max} ~ $10^{7.5}$

t_D~ 10^4 s

$$t_{\rm acc} \approx \frac{p^2}{D_p} = \frac{\rho_g(\gamma_0)}{c\ \beta_A^2} \left(\frac{B_0^2}{\delta B^2}\right)\bigg|_{\gamma_0} \left(\frac{\gamma}{\gamma_0}\right)^{2-q} .$$

evolution of the SSC SEDs vs time

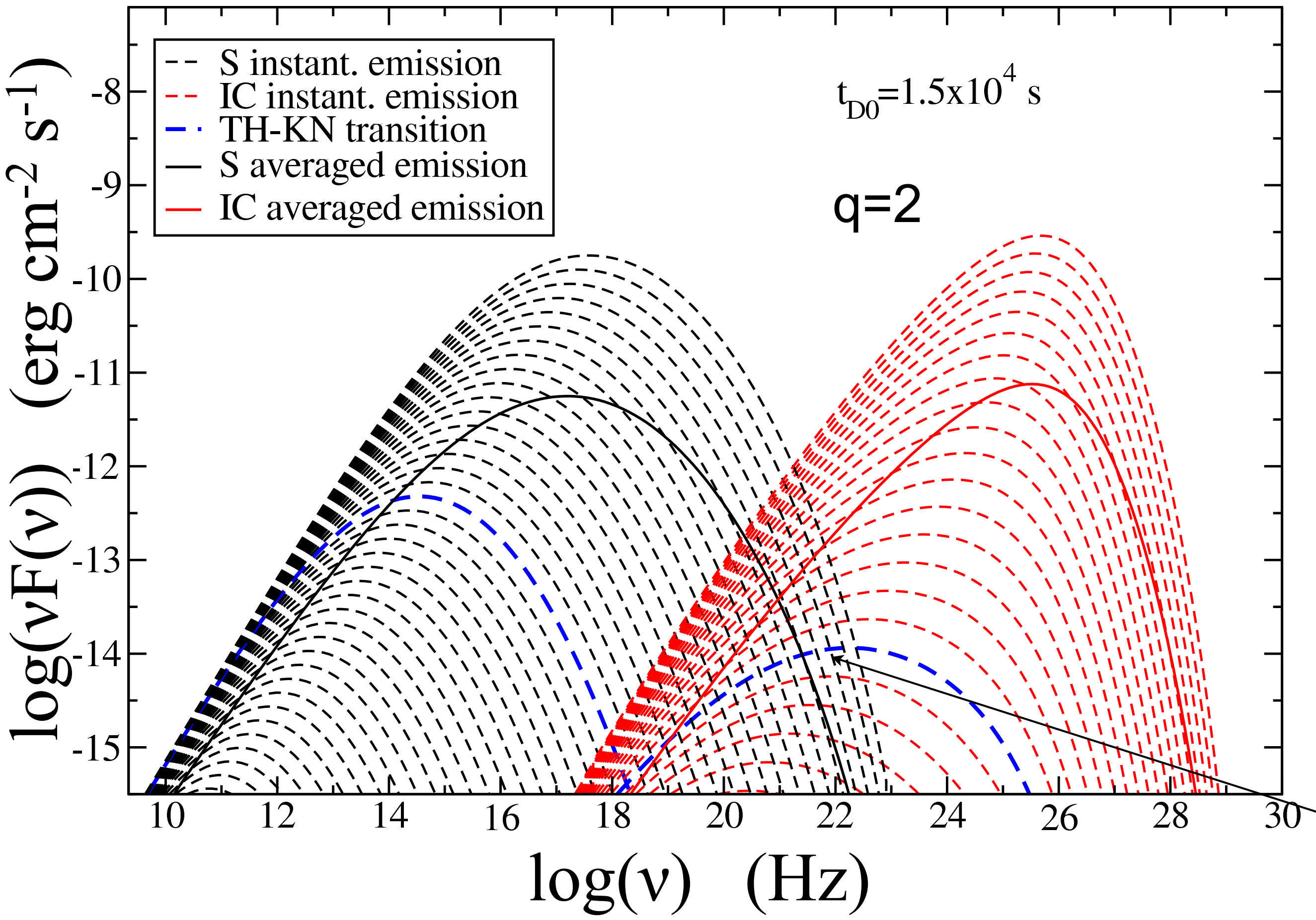

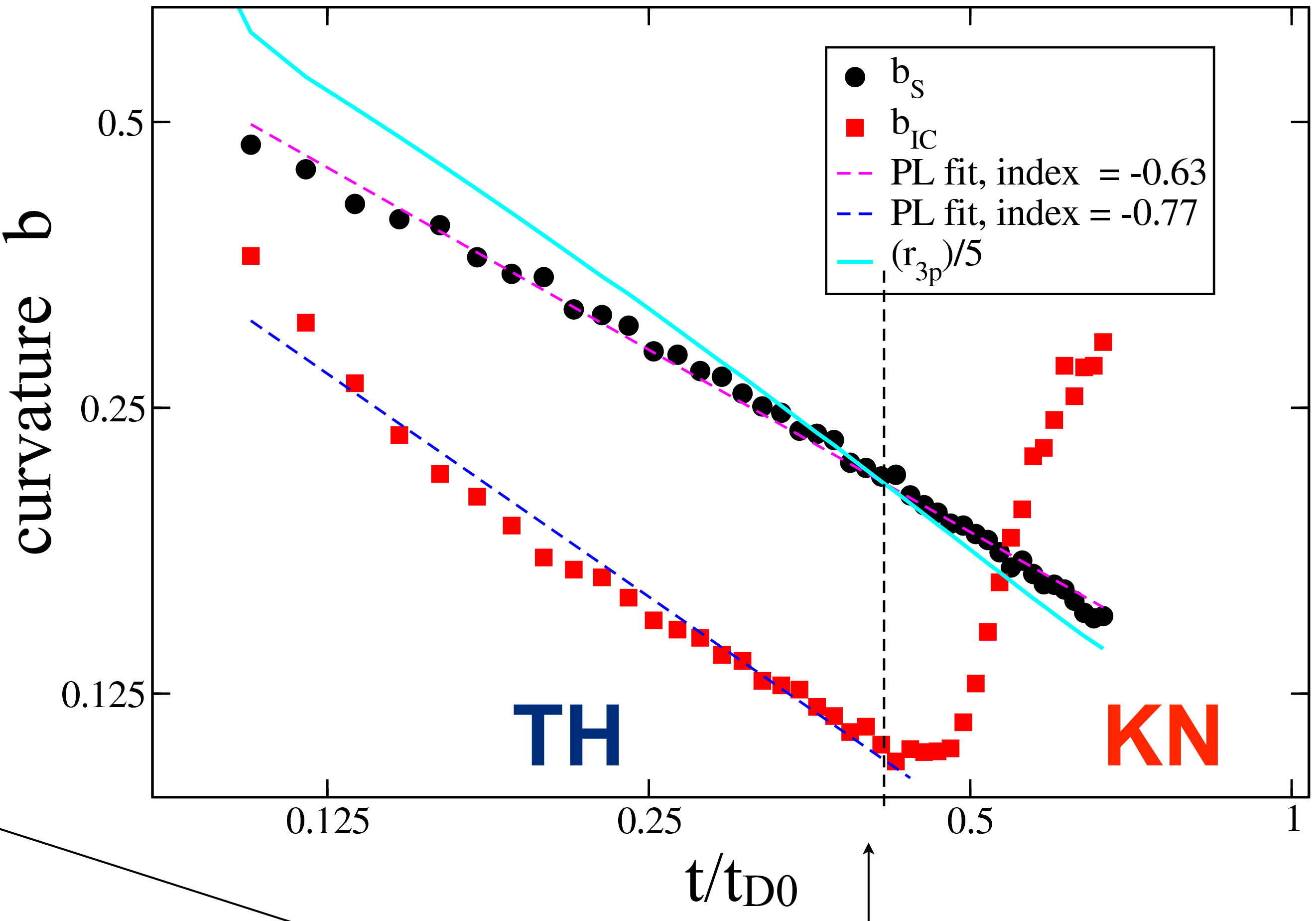

KN signature

parameter		range
R	(cm)	2×10^{15}
B	(G)	[0.01 - 1.0]
L_{inj}	(erg/s)	10^{38}
q		[3/2 - 2]
t_A	(s)	1.8×10^3
$t_{D_0} = 1/D_{P0}$	(s)	$[1.5 - 25] \times 10^4$
T_{inj}	(s)	10^4
T_{esc}	(R/c)	2.0
Duration	(s)	10^4
γ_{inj}		10.0

parameter values for n(γ) evolution study

Parameter		Impulsive Inj.		Cont. Inj.	
R	(cm)	5×10^{13}, 1×10^{15}	$\ldots$	$\ldots$	$\ldots$
B	(G)	0.1, 1.0	$\ldots$	$\ldots$	$\ldots$
$L_{\rm inj}$	(erg s^{-1})	10^{39}	$\ldots$	10^{37}	$\ldots$
q		2	3/2	2	3/2
$t_{D_0} = 1/D_{P0}$	(s)	1×10^4	1×10^3	1×10^4	1×10^3
$T_{\rm inj}$	(s)	100	$\ldots$	1×10^4	$\ldots$
$T_{\rm esc}$	(R/c)	∞	$\ldots$	2	$\ldots$
Duration	(s)	1×10^5	$\ldots$	$\ldots$	$\ldots$
$\gamma_{\rm inj}$		10.0	$\ldots$	10.0	$\ldots$

Size effect on IC cooling, R~ 5x10^{13} cm, q=2

R= 1x10^{15} cm

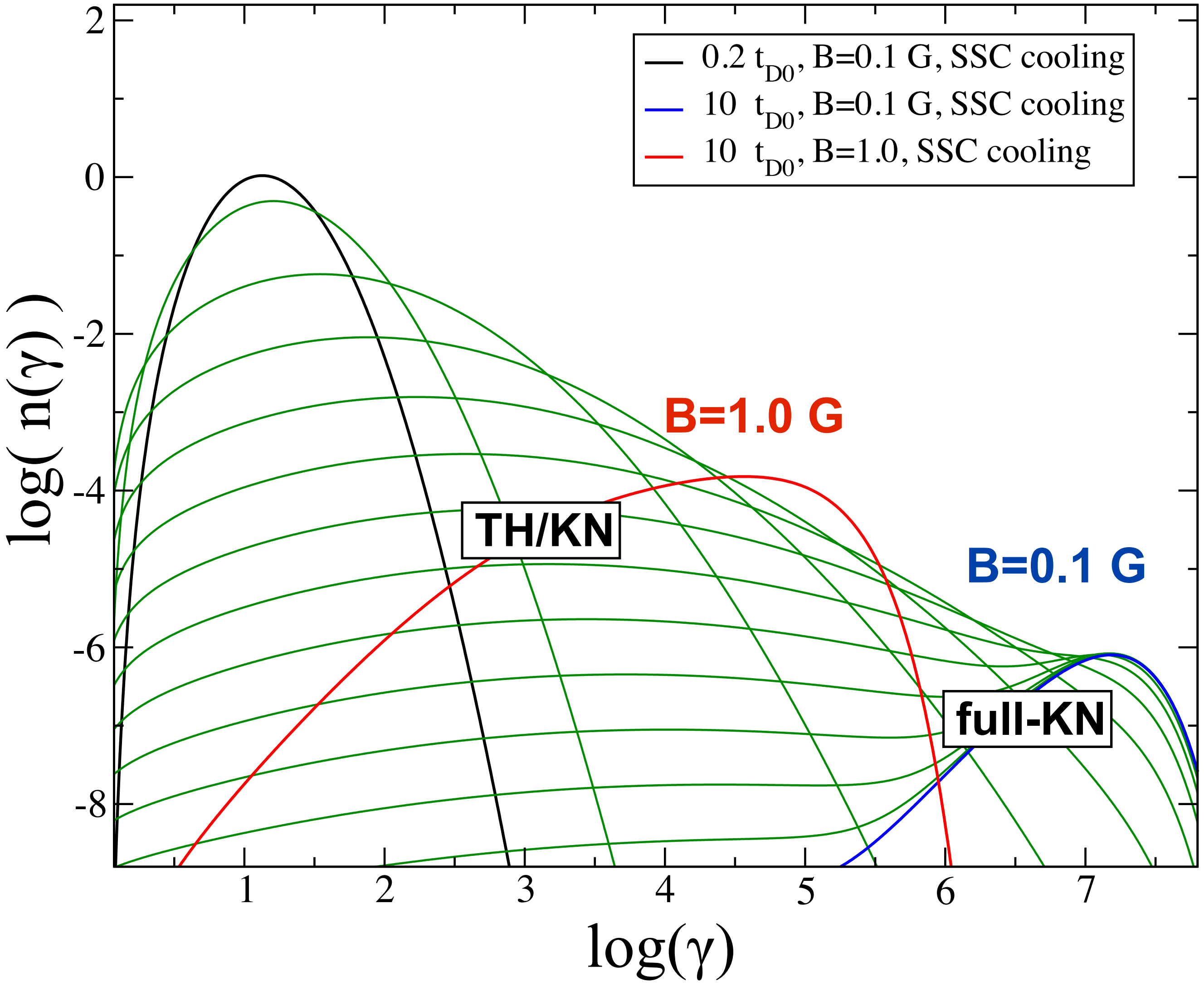

R= 5x10^{13} cm

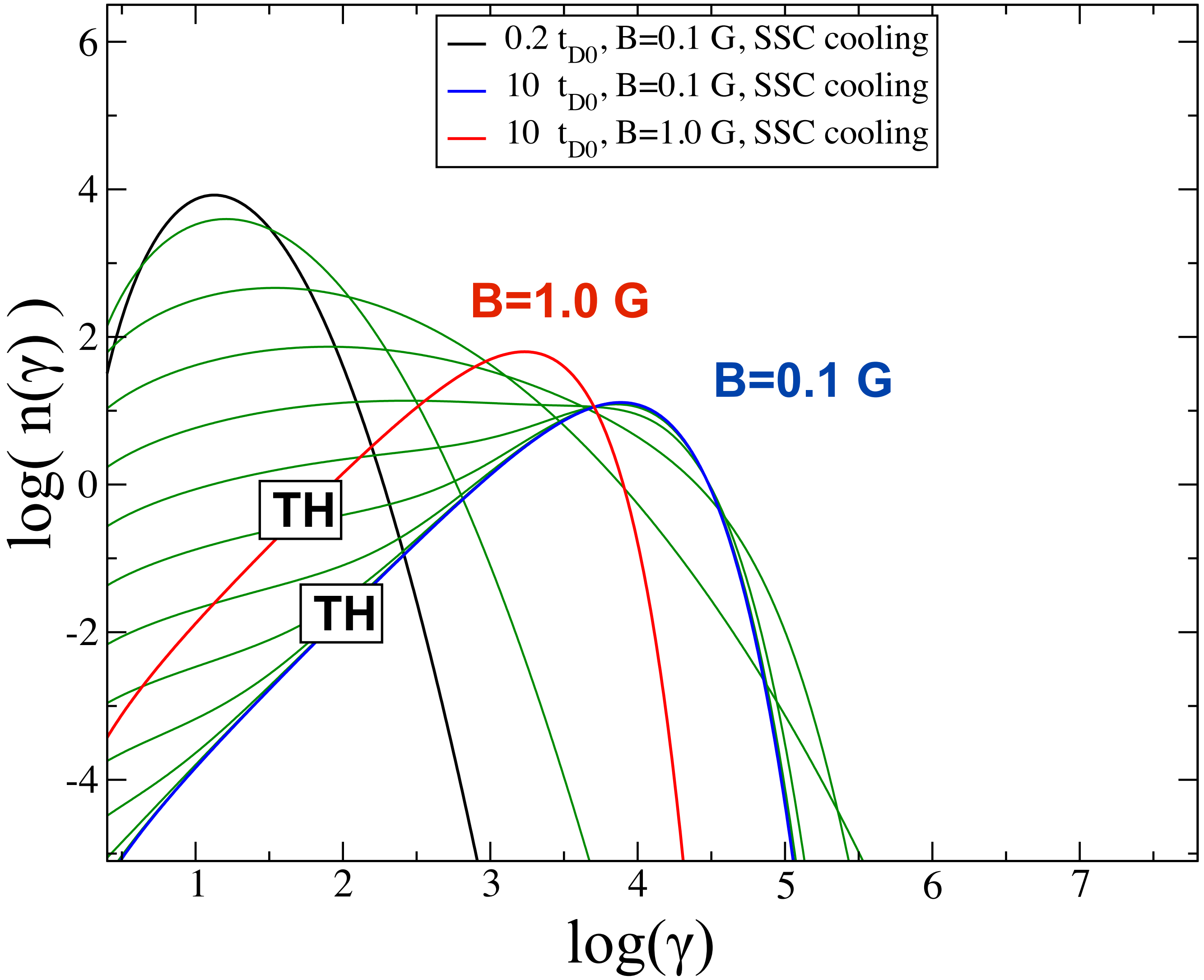

U$_{ph}$ (R= 1x10^{13} cm) **>> U$_{ph}$** (R= 5x10^{15} cm)

IC prevents higher energies in more compact accelerators (if all the parameters are the same)

impulsive injection

$q=3/2$, $R=10^{15}$ cm, $B=0.1$ G $t_{inj}=t_D(\gamma_{inj})10^3$ s

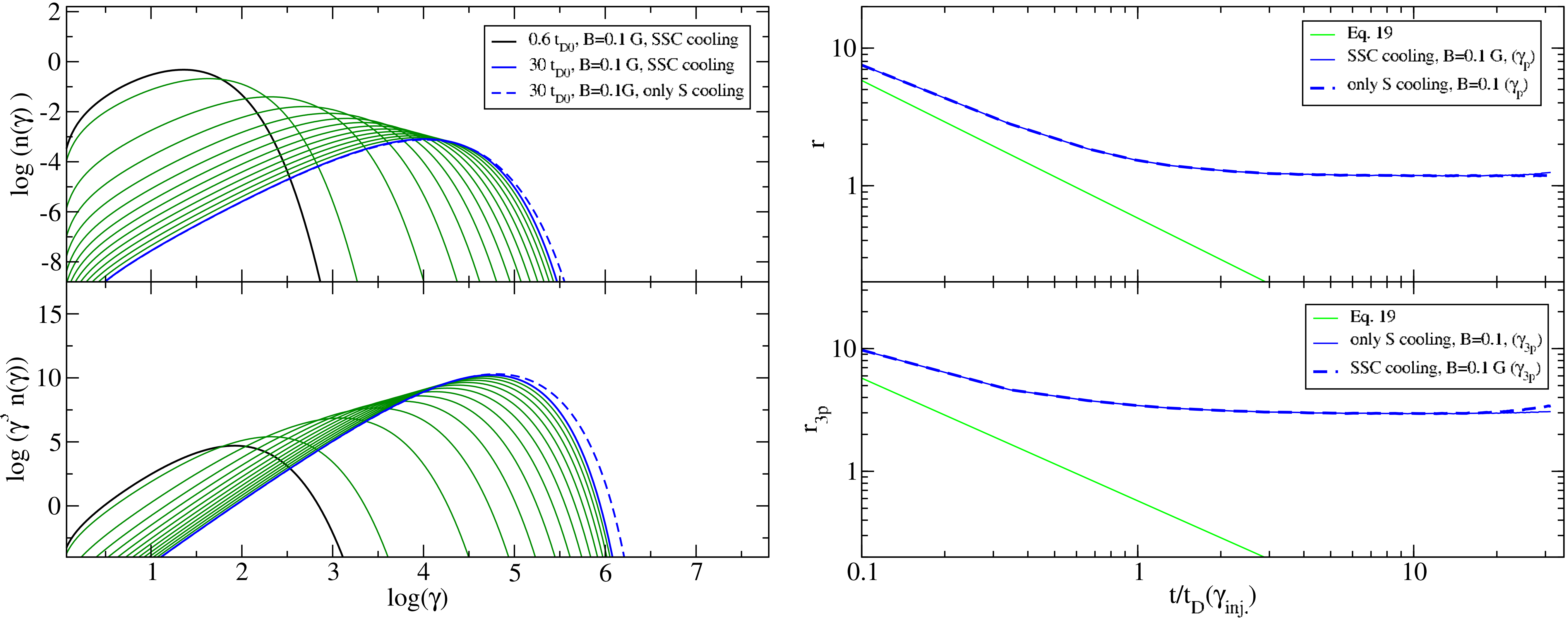

- t_D energy-dep. increasing with γ
- eq-energy lower compared to $q=2$
- curvature milder

A. Spitkovsky 2008 ApJ 682:L5-L8

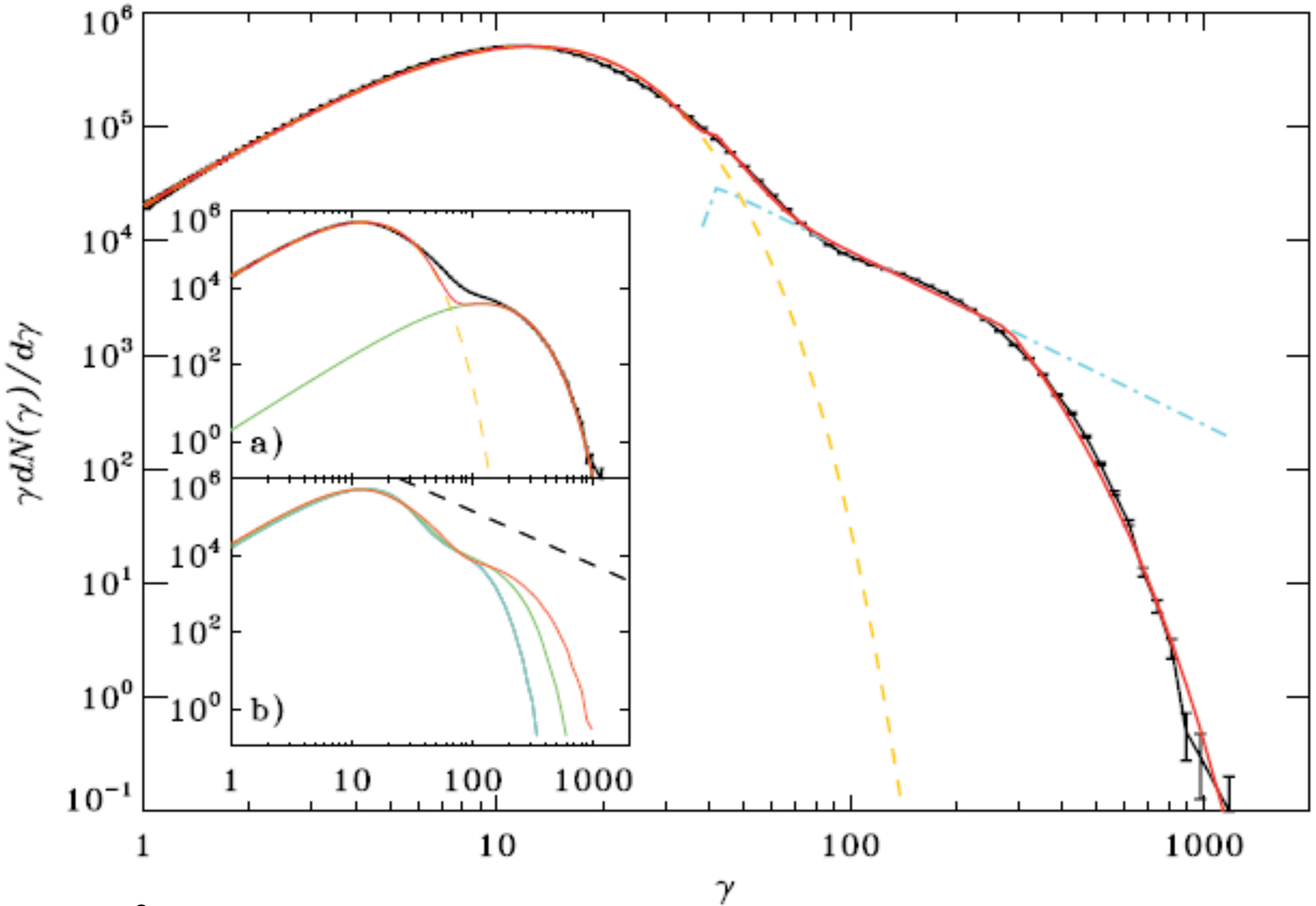

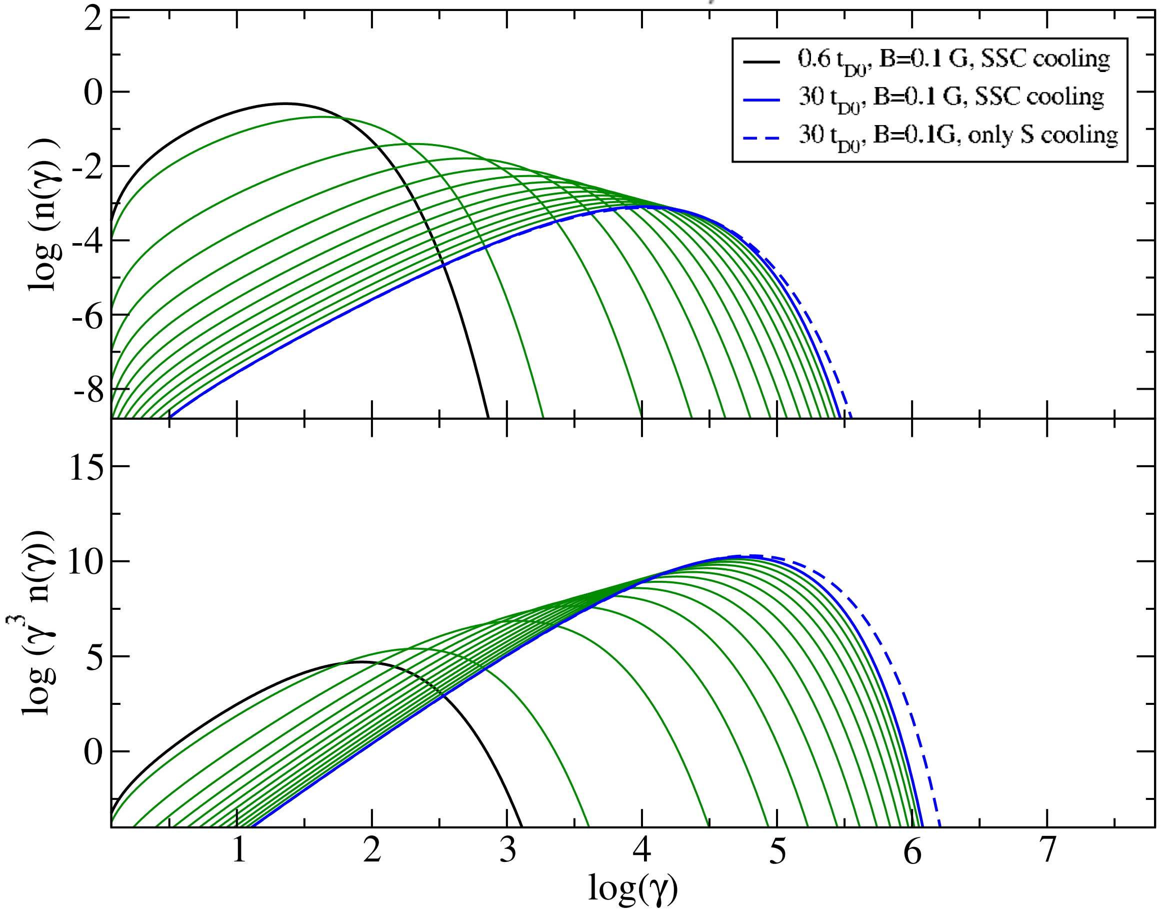

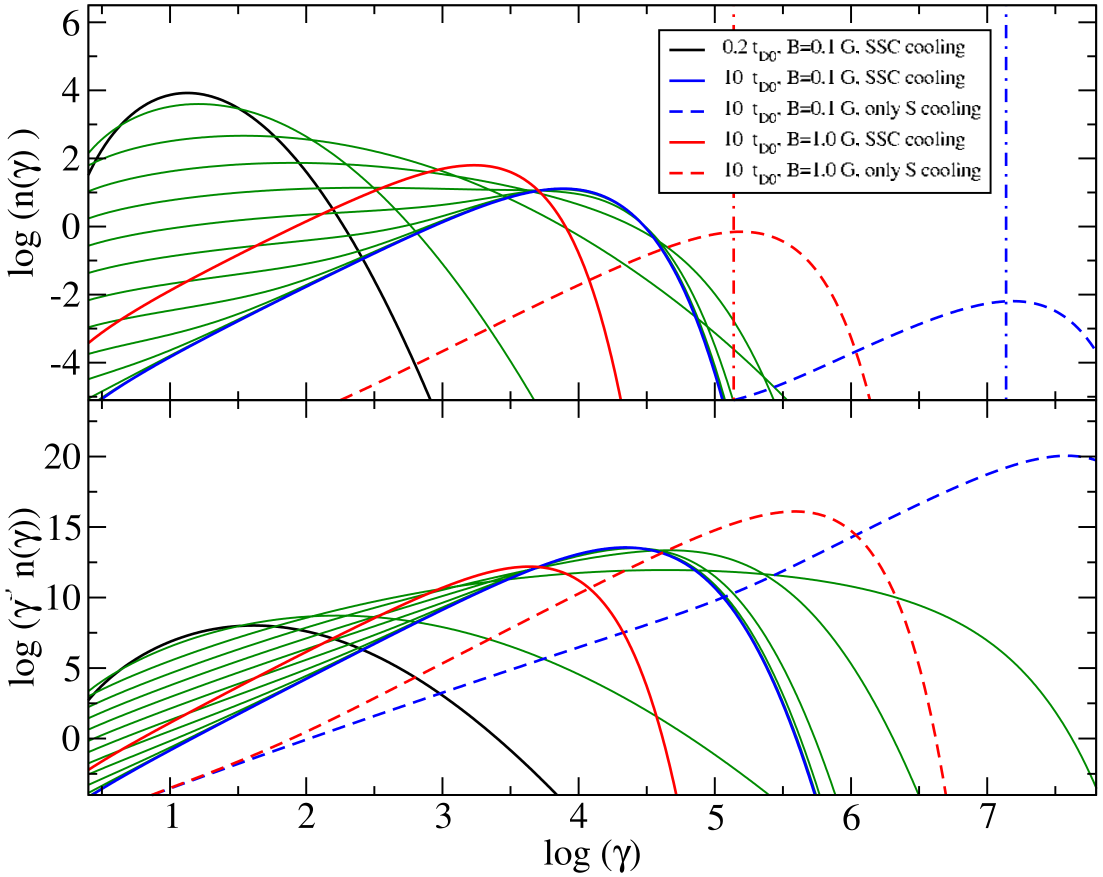

Cooling rates at the final step of the temporal evolution

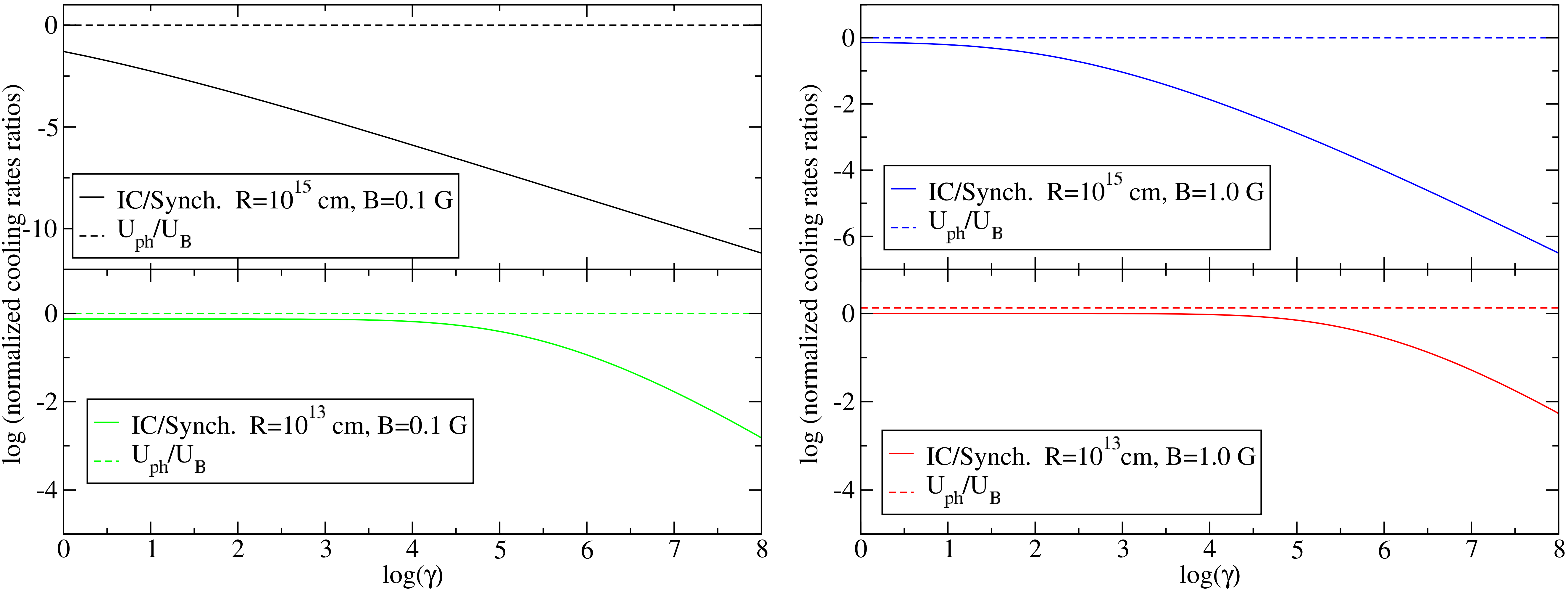

$$\gamma_{\rm eq} = \frac{1}{t_{\rm acc} C_0 (U_B + F_{\rm KN}(\gamma))}$$

IC dominated

$$\gamma_{\rm eq} \propto (R^2 / t_{\rm acc} B^2 f_{\rm KN})$$

KN/Synch dominated

$$\gamma_{\rm eq} \propto (1/t_{\rm acc} B^2)$$

Continuous injection
q=2, R=10^{15} cm, B=0.1 G, t_{inj}=t_D=10^4 s

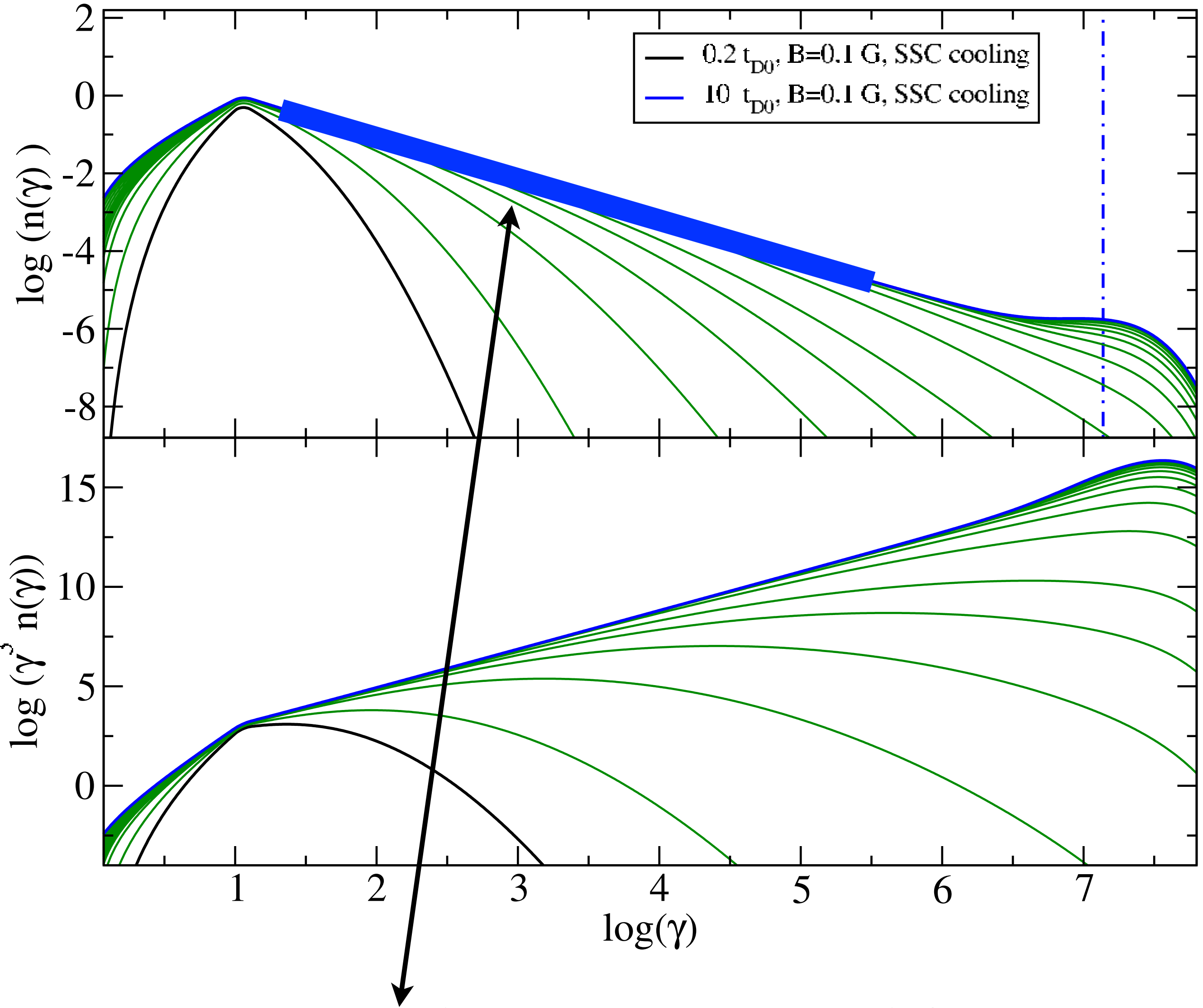

PL~1.06, in agreement with 1+$t_{min-acc}/2t_{esc}$

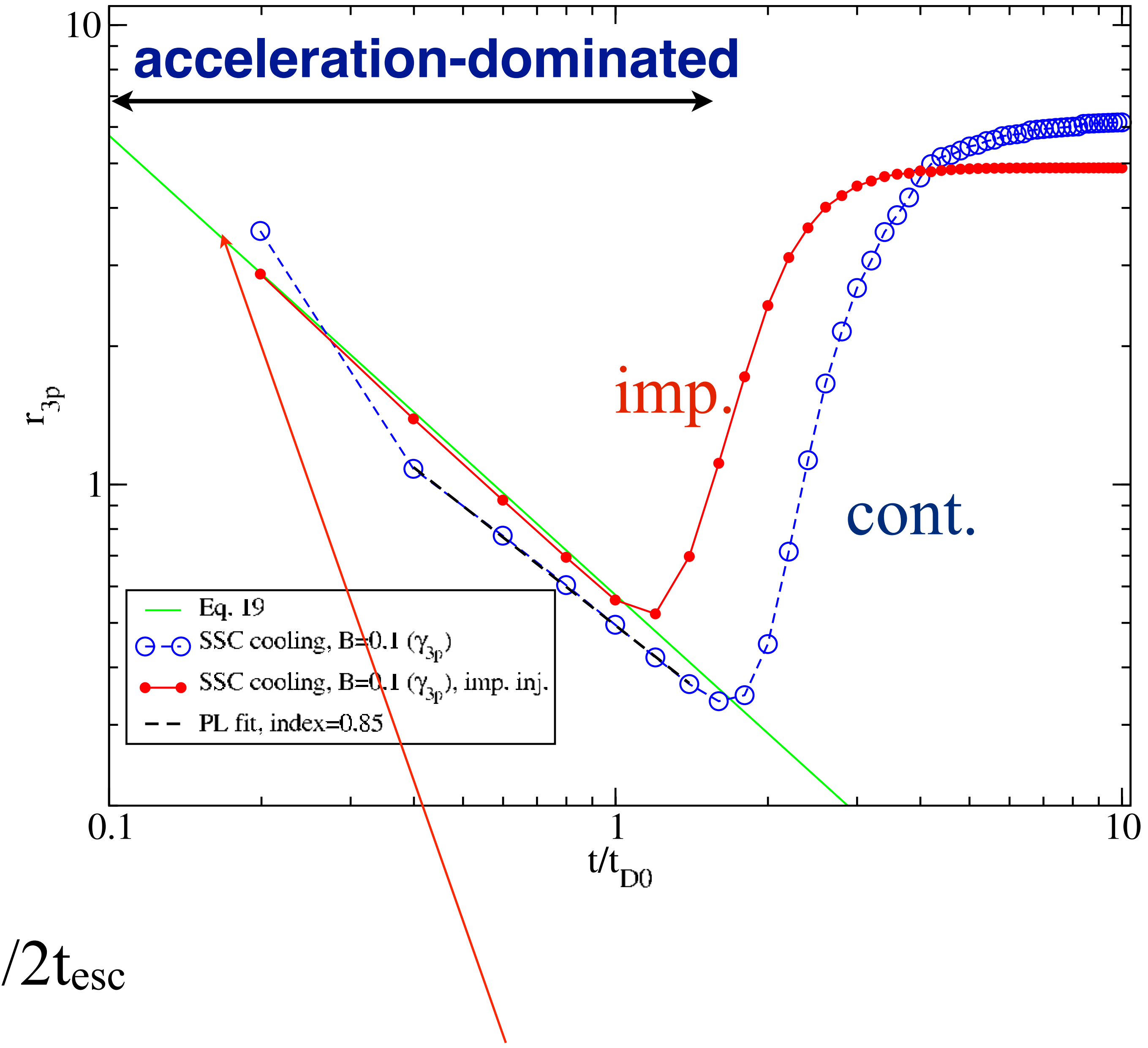

$$r = \frac{c_e}{4D_{p0}\ t} \propto \frac{1}{D_{p0}t}$$

parameter values for SEDs evolution study

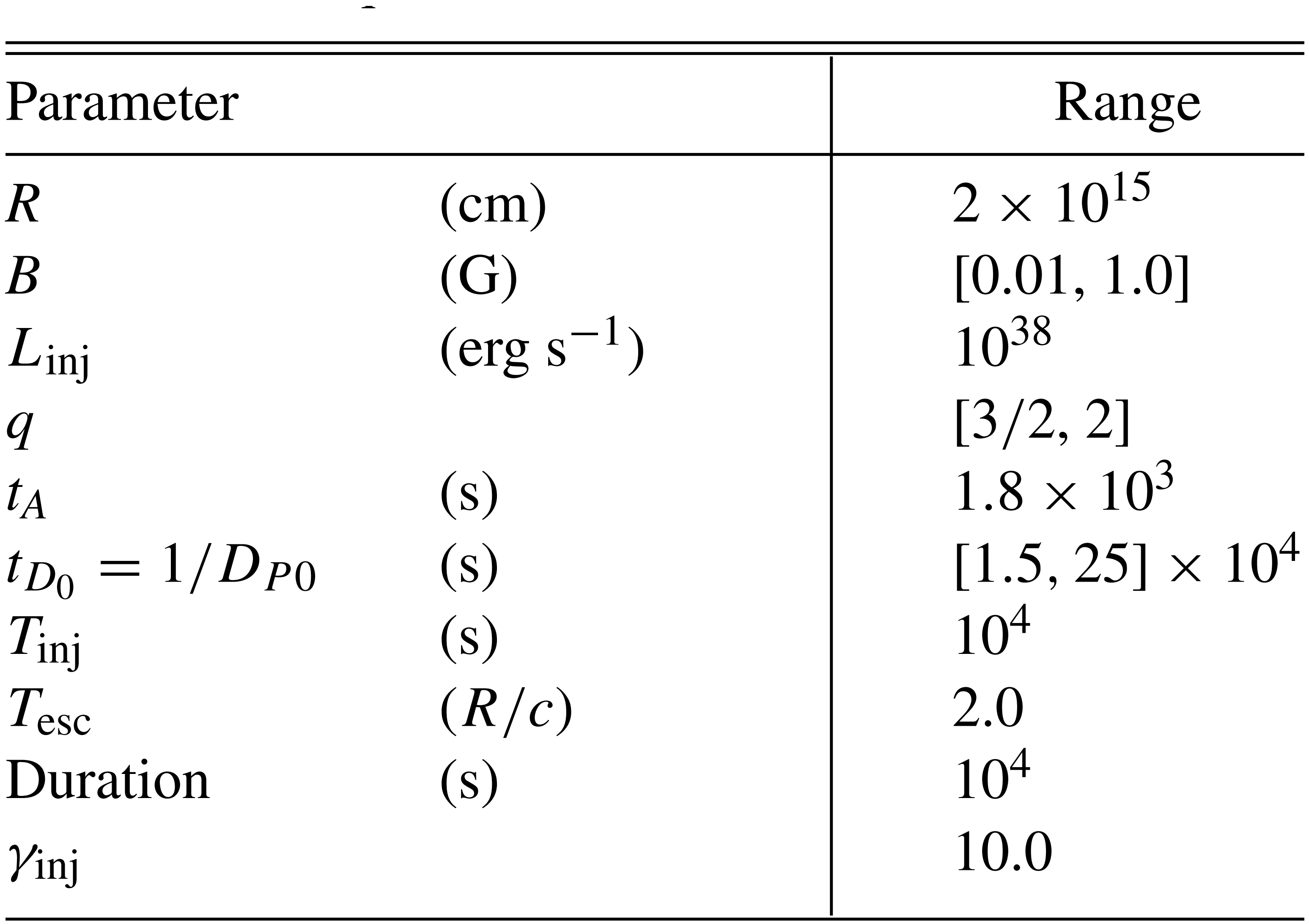

Parameter		Range
R	(cm)	2×10^{15}
B	(G)	[0.01, 1.0]
$L_{\rm inj}$	(erg s^{-1})	10^{38}
q		[3/2, 2]
t_A	(s)	1.8×10^3
$t_{D_0} = 1/D_{P0}$	(s)	$[1.5, 25] \times 10^4$
$T_{\rm inj}$	(s)	10^4
$T_{\rm esc}$	(R/c)	2.0
Duration	(s)	10^4
$\gamma_{\rm inj}$		10.0

evolution of the SSC SEDs

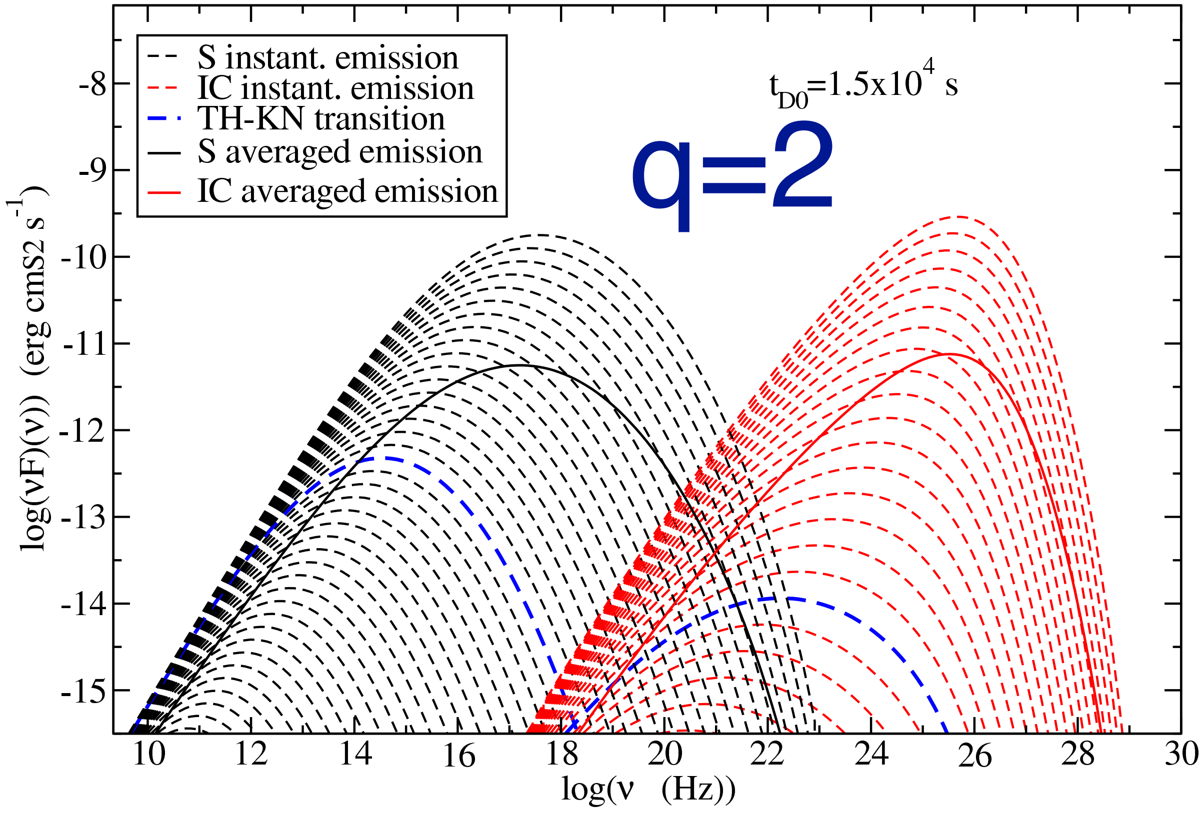

q=2

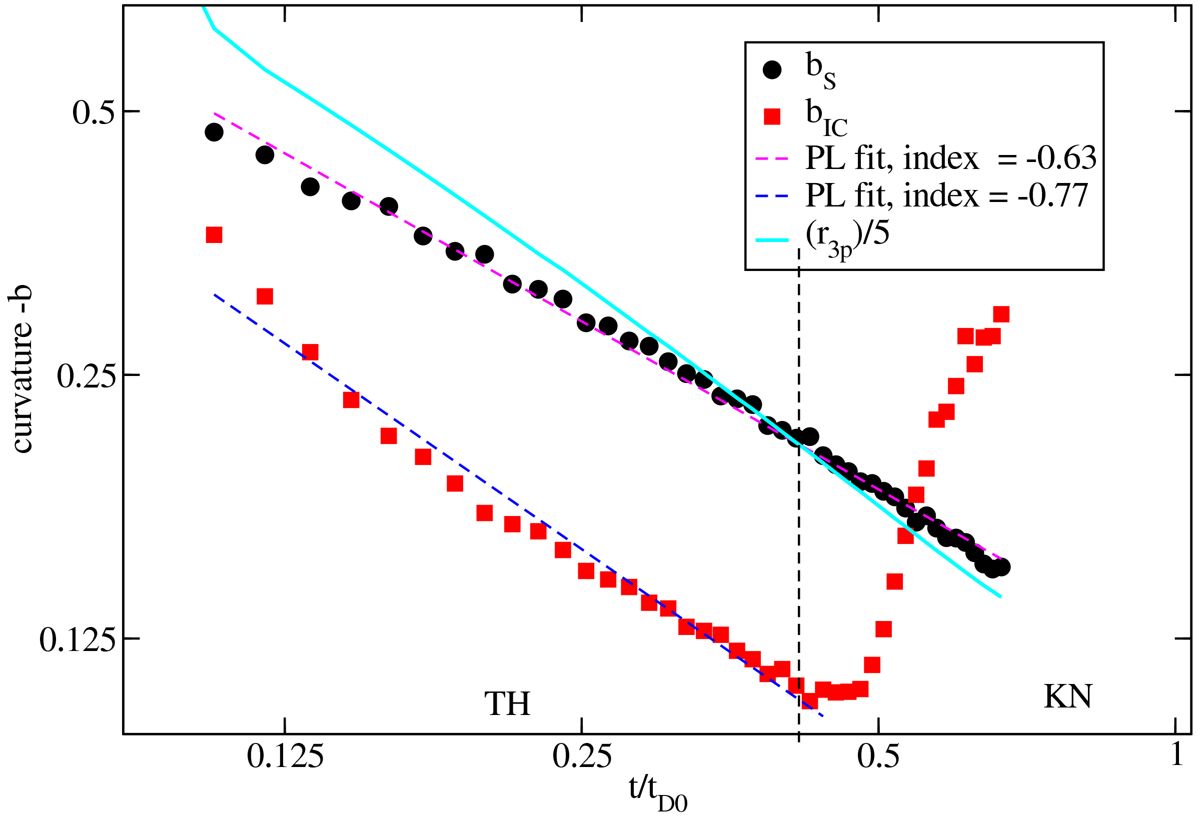

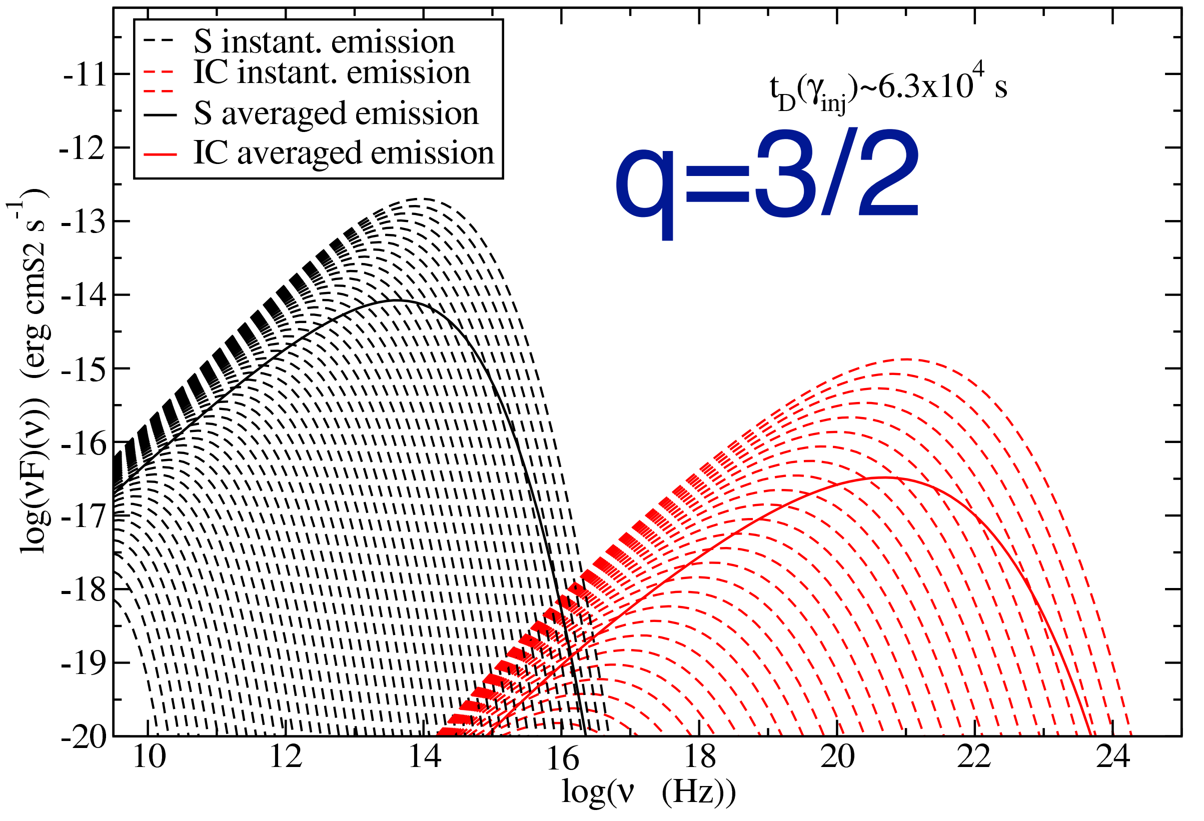

q=3/2

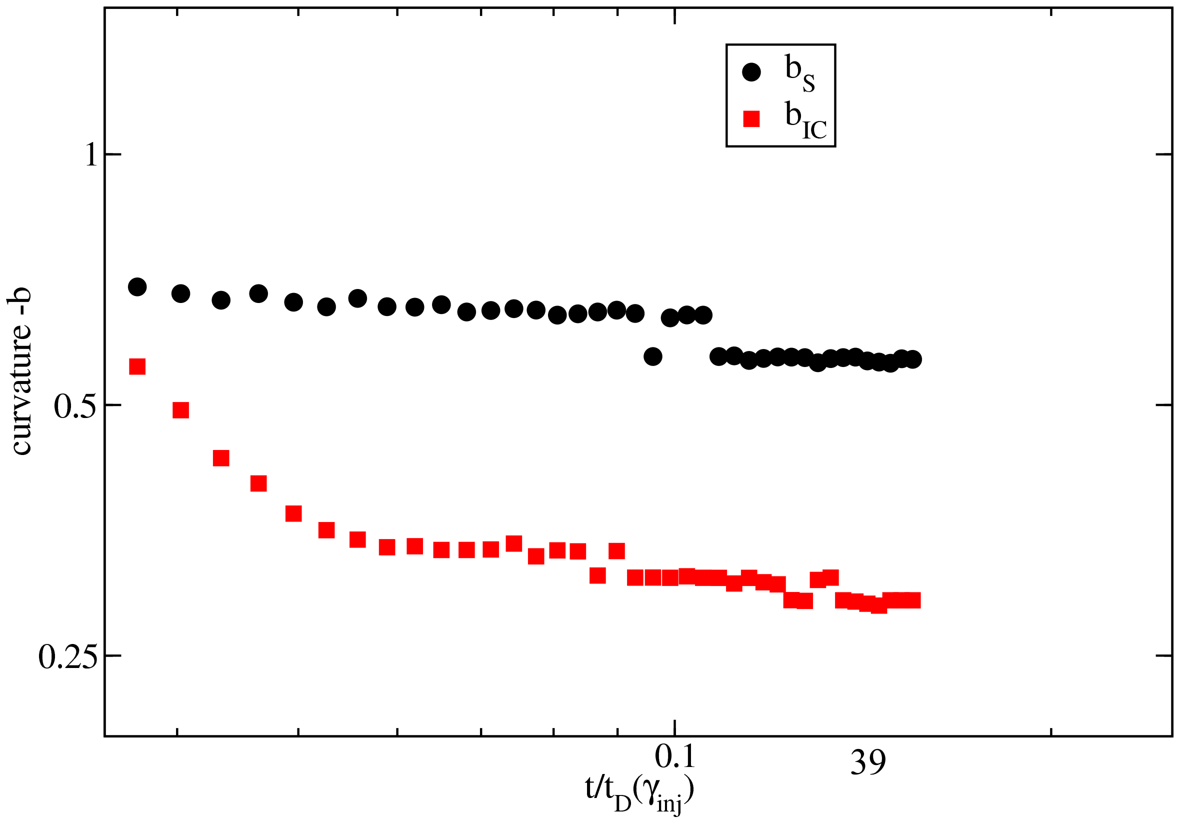

D_p-driven trends t_D=[$1.5x10^4$-$1.5x10^5$]s

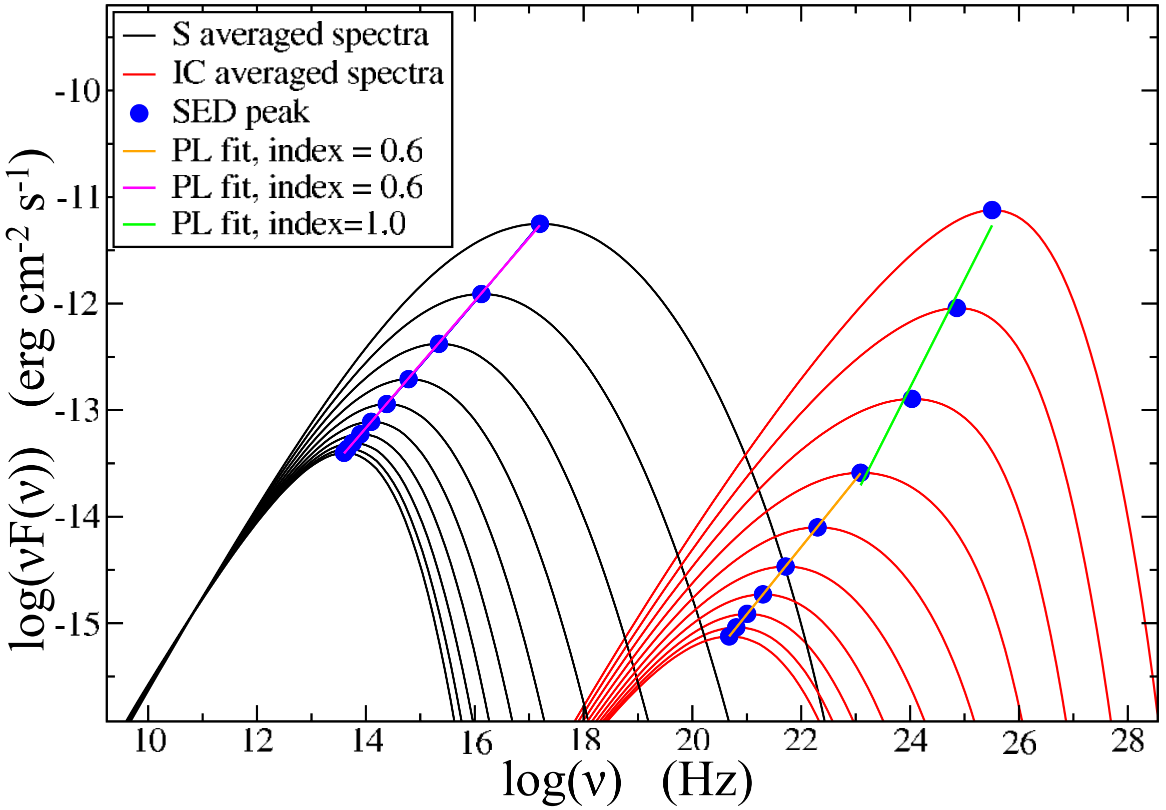

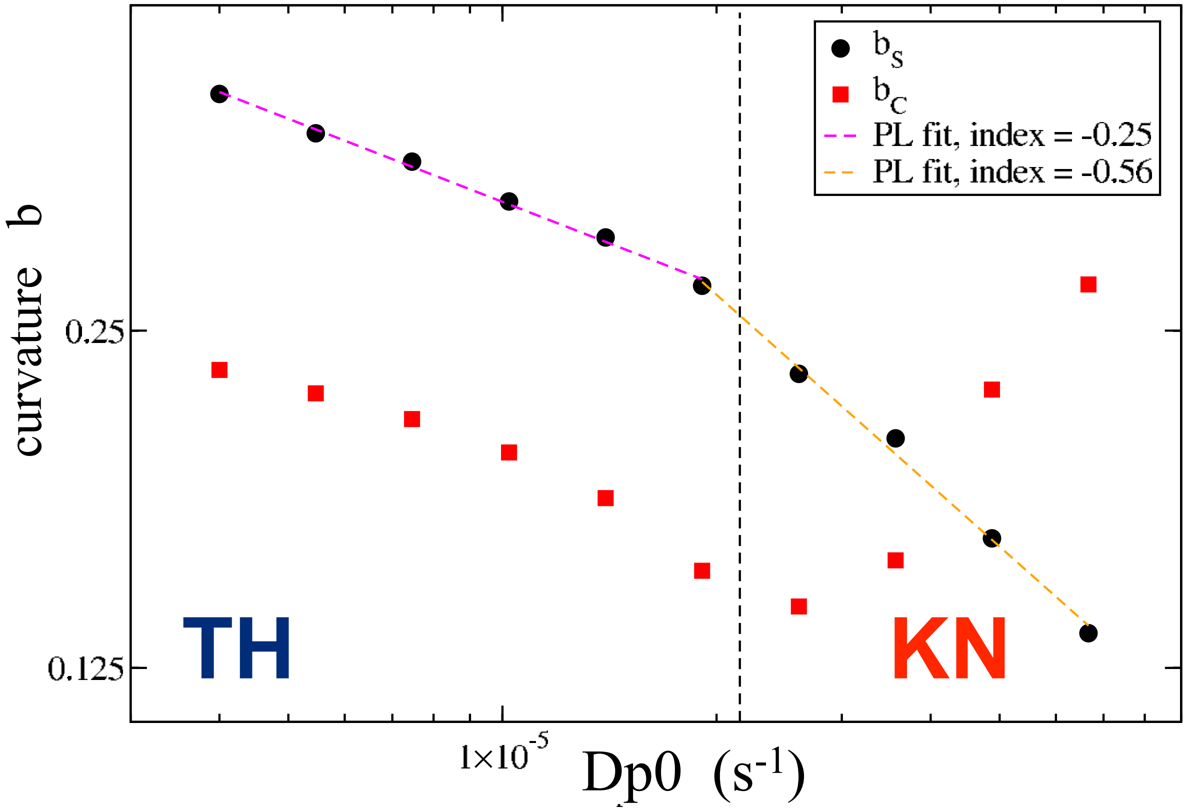

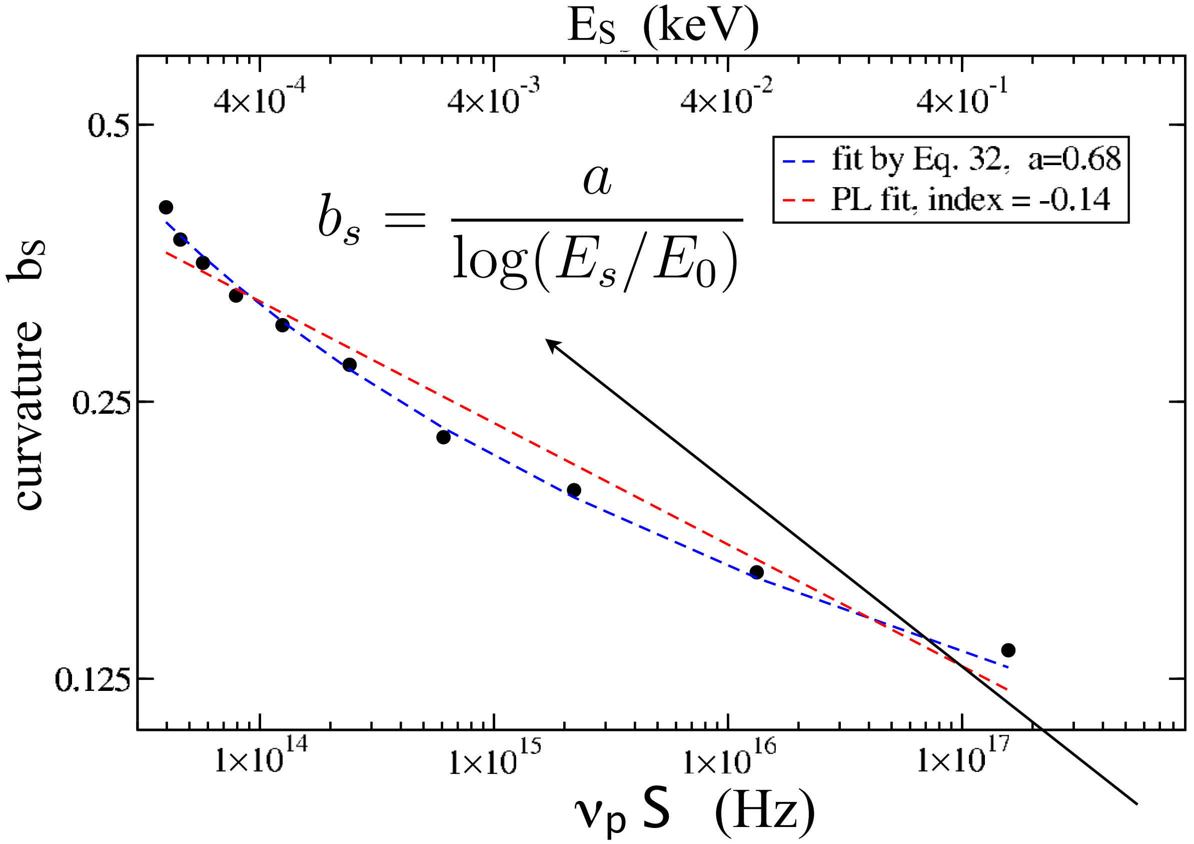

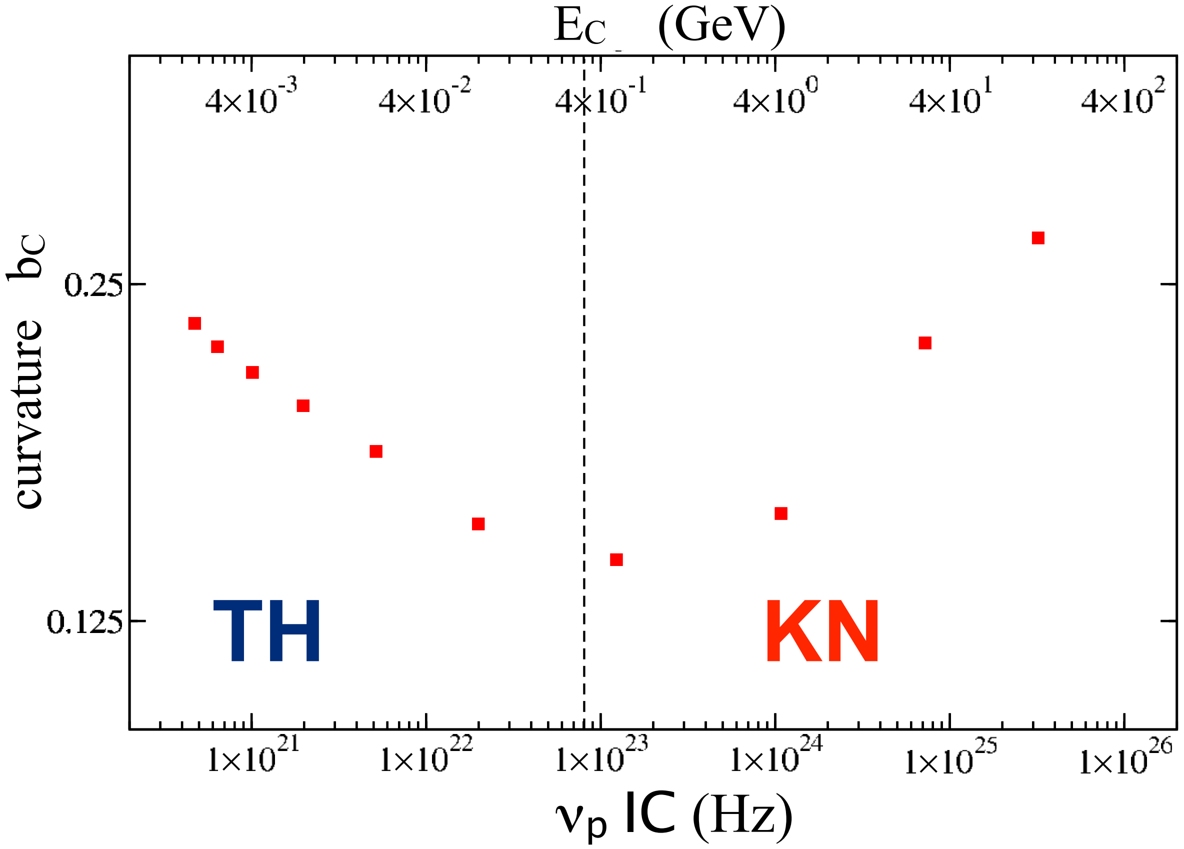

$$\boxed{\log(\gamma_{3p}) = \log(\gamma_p) + \frac{3}{2r} \longrightarrow \log(E_s) \propto 2\log(\gamma_p) + \frac{3}{5b}}$$

B-driven trends

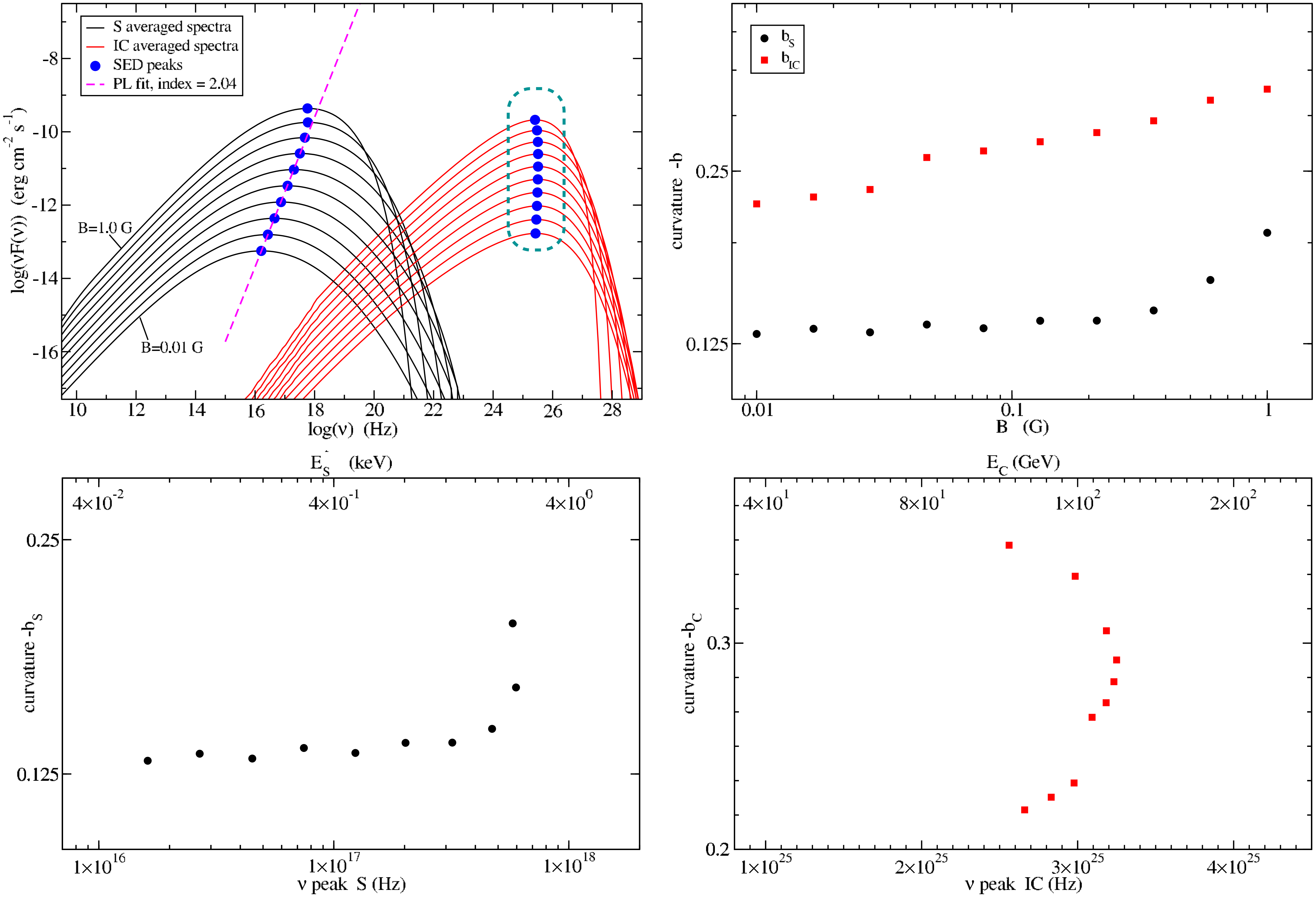

parameter values for X-ray trends reproduction

Parameter		D Trend	q Trend
R	(cm)	3×10^{15}	...
B	(G)	[0.05, 0.2]	...
$L_{\rm inj}$ (E_s–b_s trend)	(erg s^{-1})	5×10^{39}	...
$L_{\rm inj}$ (E_s–L_s trend)	(erg s^{-1})	5×10^{38}, 5×10^{39}	...
q		2	[3/2, 2]
t_A	(s)	1.2×10^3	...
$t_{D_0} = 1/D_{P0}$	(s)	$[1.5 \times 10^4, 1.5 \times 10^5]$	1.5×10^4
$T_{\rm inj}$	(s)	10^4	...
$T_{\rm esc}$	(R/c)	2.0	...
Duration	(s)	10^4	...
$\gamma_{\rm inj}$		10.0	...

E_s-b_s: Comparison with the data

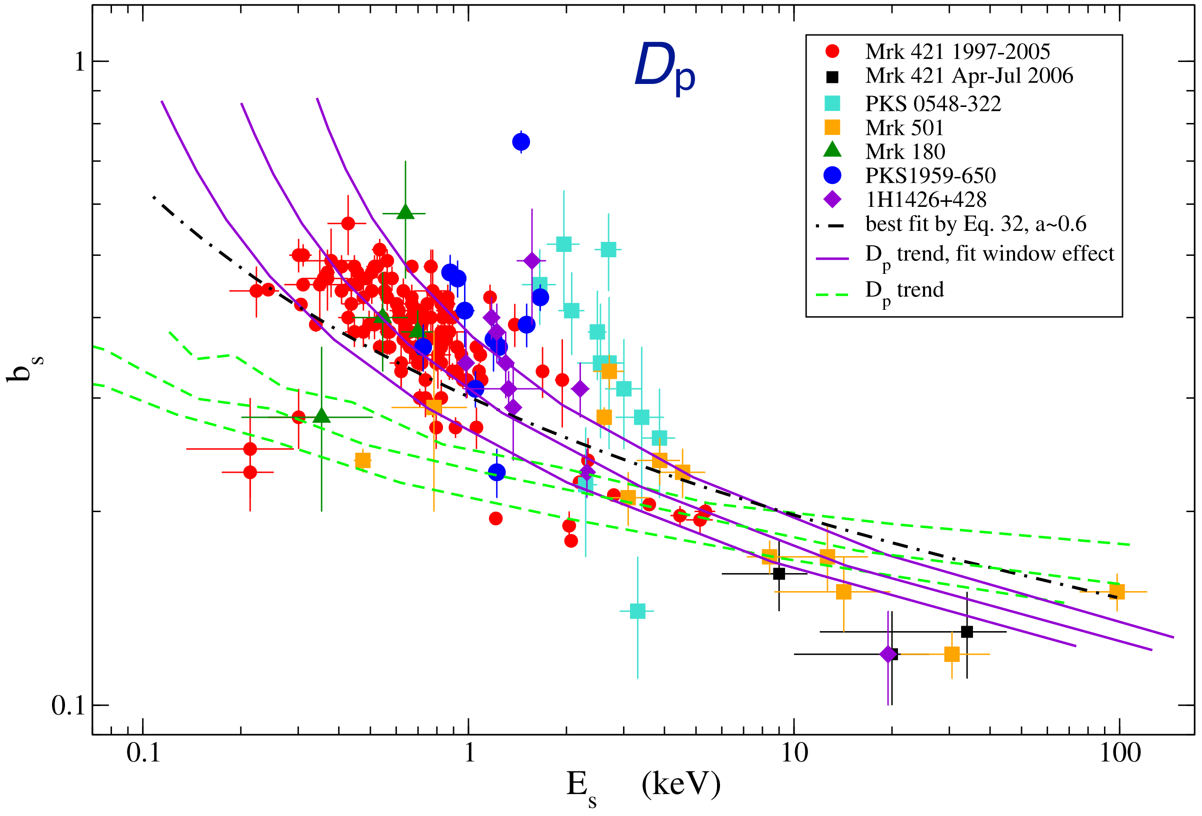

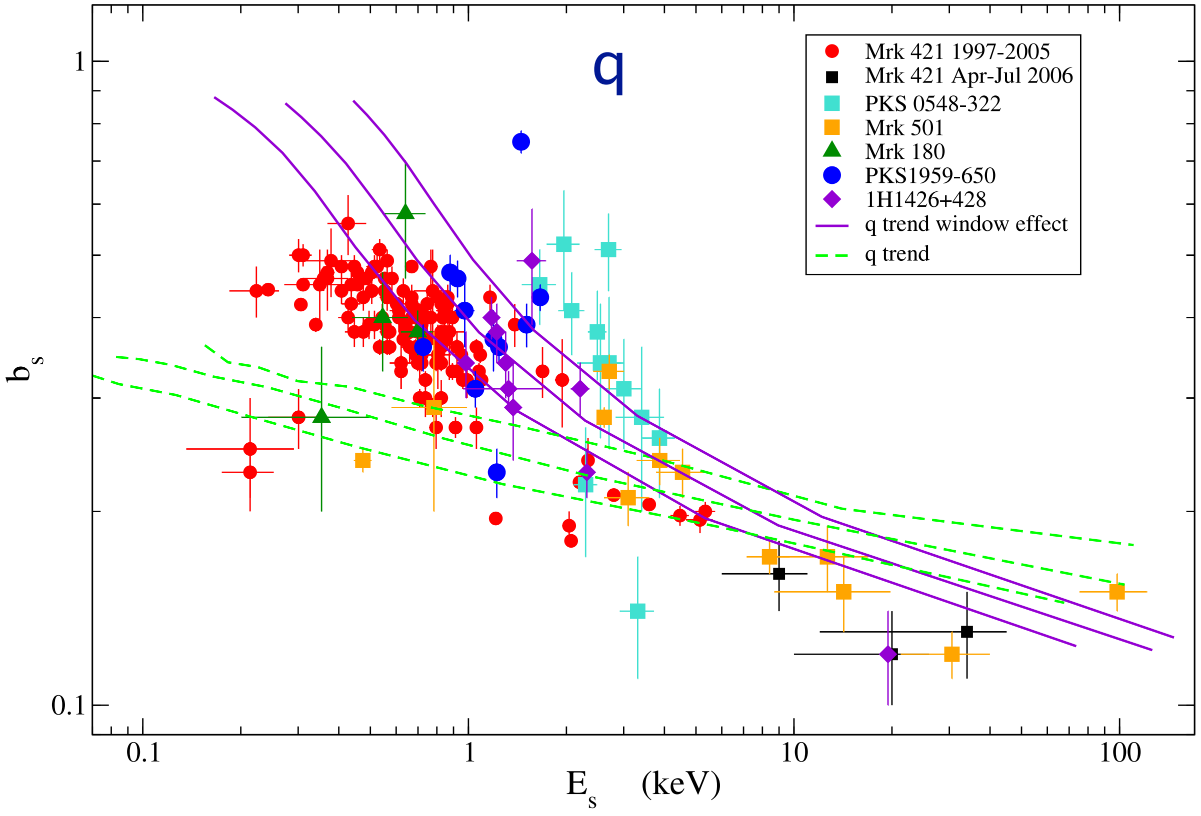

		$\hat{D}$ trend	q trend
R	(cm)	3×10^{15}	-
B	(G)	[0.05-0.2]	-
L_{inj} (**E_s-b_s trend**)	(erg/s)	5×10^{39}	-
L_{inj} (**E_s-L_s trend**)	(erg/s)	$\mathbf{5 \times 10^{38}}$, $\mathbf{5 \times 10^{39}}$	-
q		2	[3/2-2]
t_A	(s)	1.2×10^3	-
$t_{D_0} = 1/D_{P0}$	(s)	$[1.5 \times 10^4 - 1.5 \times 10^5]$	1.5×10^4
T_{inj}	(s)	10^4	-
T_{esc}	(R/c)	2.0	-
Duration	(s)	10^4	-
γ_{inj}		10.0	-

- two scenarios, D_p–driven and q–driven
- data span 13 years, both flaring and quiescent states
- We are able to reproduce these long-term behaviors, by changing the value of only one parameter (D_p or q)
- for q=2, curvature values imply distribution far from the equilibrium (b~1.2)
- for q=3/2, curvature values are compatible with the equilibrium (b~0.6) only for Es<~ 1.5 keV

E_S-L_S: Comparison with the data

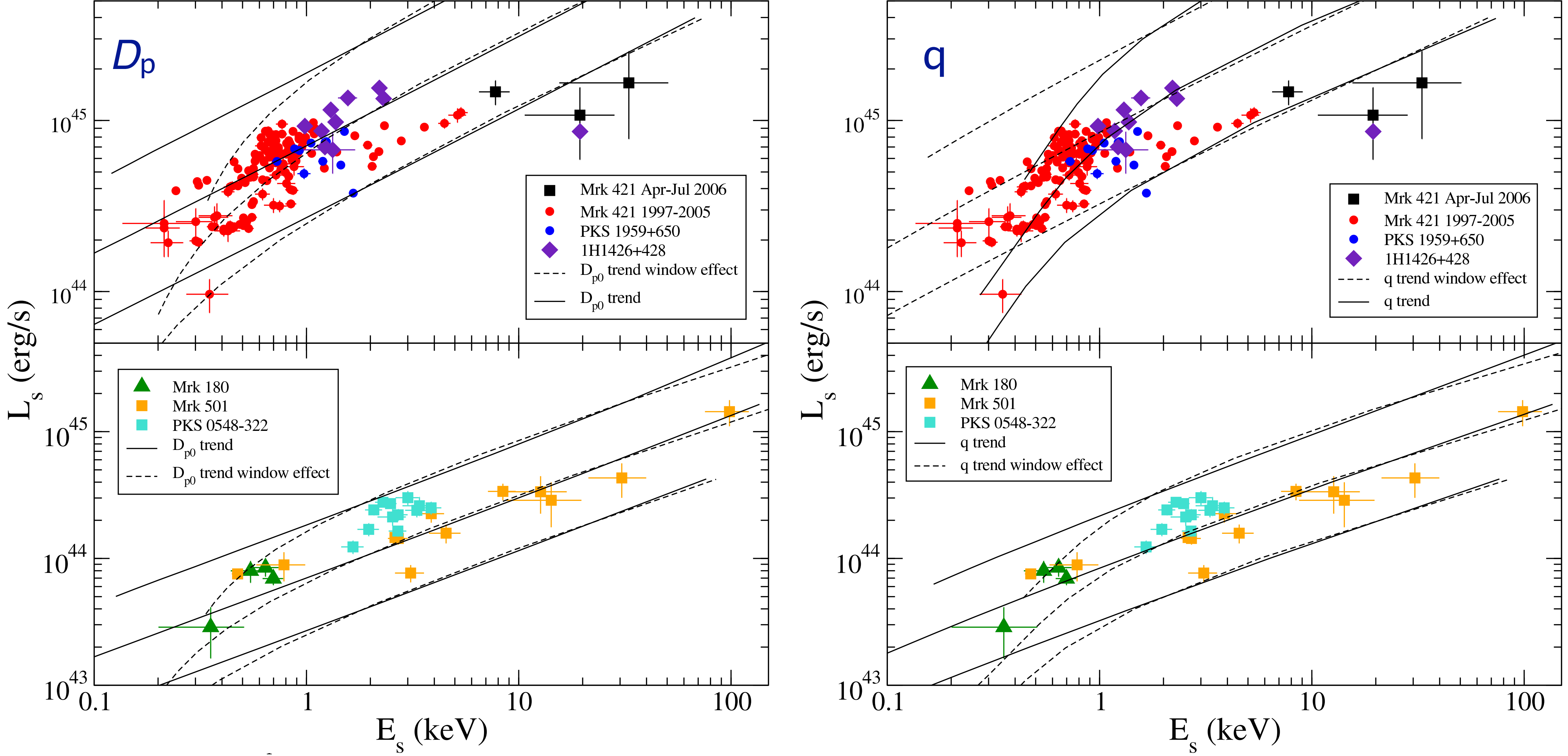

		D trend	q trend
R	(cm)	3×10^{15}	-
B	(G)	[0.05-0.2]	-
L_{inj} (**E_s-b_s trend**)	(erg/s)	5×10^{39}	-
L_{inj} (**E_s-L_s trend**)	(erg/s)	$\mathbf{5 \times 10^{38}, 5 \times 10^{39}}$	-
q		2	[3/2-2]
t_A	(s)	1.2×10^3	-
$t_{D_0} = 1/D_{P0}$	(s)	$[1.5 \times 10^4 - 1.5 \times 10^5]$	1.5×10^4
T_{inj}	(s)	10^4	-
T_{esc}	(R/c)	2.0	-
Duration	(s)	10^4	-
γ_{inj}		10.0	-

- the E_S-S_S (E_S-L_S) relation follows naturally from that between E_S and b_S

- the average index of the trend $L_S \propto E_S^{\alpha}$ with a~0.6 is compatible with the data, and with a scenario in which a typical luminosity is injected for any flare (jet-feeding problem), whilst the peak dynamic is ruled by the turbulence in the magnetic field.